Marco M., Rodríguez-Millán M., Santiuste, C., Giner, E., Miguélez, H. A review on recent advances in numerical modelling of bone cutting, Journal of the Mechanical Behavior of Biomedical Materials, Volume 44, April 2015, Pages 179–201. Avalaible in http://dx.doi.org/10.1016/j.jmbbm.2014.12.006

A review on recent advances in numerical modelling of bone cutting

Miguel Marco[a], *Marcos Rodríguez-Millán*[a], *Carlos Santiuste*[b], *Eugenio Giner*[c], *María Henar Miguélez*[a,*]

[a]*Department of Mechanical Engineering, University Carlos III of Madrid, Avda. de la Universidad 30, 28911 Leganés, Madrid, Spain*

[b]*Department of Continuum Mechanics and Structural Analysis, University Carlos III of Madrid, Avda. de la Universidad 30, 28911 Leganés, Madrid, Spain*

[c]*Department of Mechanical and Materials Engineering (CIIM), Universitat Politècnica de València, Camino de Vera,*46022 Valencia, *Spain*

Abstract: ommon practice of surgical treatments in orthopaedics and traumatology involves cutting processes of bone. These operations introduce risk of thermo-mechanical damage, since the threshold of critical temperature producing thermal osteonecrosis is very low. Therefore, it is important to develop predictive tools capable of simulating accurately the increase of temperature during bone cutting, being the modelling of these processes still a challenge. In addition, the prediction of cutting forces and mechanical damage is also important during machining operations. As the accuracy of simulations depends greatly on the proper choice of the thermo-mechanical properties, an essential part of the numerical model is the constitutive behaviour of the bone tissue, which is considered in different ways in the literature. This paper focuses on the review of the main contributions in modelling of bone cutting with special attention to the bone mechanical behaviour. The aim is to give the reader a complete vision of the approaches commonly presented in the literature in order to help in the development of accurate models for bone cutting.

Keywords: Cortical bone, Mechanical behaviour, Cutting processes, Numerical modelling.

1. Introduction

General orthopaedic and traumatologic surgery and dentistry commonly involve cutting of bone. Cutting operations entail a wide range of processes covering sawing (James et al., 2014), drilling (Fox et al., 2013) and grinding (Tai et al., 2013).

The well-known industrial concepts of productivity and surface integrity in material removal processes can be translated to medical applications. In this surgical context reduced cutting time is related to short surgery global time and bone integrity is related to the absence of cutting induced damage, mainly thermal osteonecrosis. Thermal necrosis, induced due to excessive temperature, is the main risk for the bone tissue surrounding the cutting zone. Further clinical problems such as loosening of implant interfaces could be derived from thermal necrosis during surgery. The importance of this problem has motivated the development of different research works focusing on the problem of osteonecrosis caused by bone cutting during surgery. Recent reviews dealing with bone drilling, a common operation for screw accommodation, are presented in Augustin et al., 2012; Pandey and Panda, 2013.

Despite the interest of works dealing with bone cutting, it is really difficult to extract from them concluding remarks. The main reason is the wide variety of parameters involved in heat generation during cutting, such as the tool geometry, the cutting parameters or the use of coolant, which are different in each application analysed in the literature. On the other hand in-process monitoring of temperature is still a challenge at present.

The modelling of cutting processes can help in the understanding of bone cutting and thus in the analysis and definition of cutting operations in bones. Validated models allow to obtain information about variables that are difficult to measure. Accuracy of the model predictions rely on the proper definition of the type of approach, geometry, boundary conditions, constitutive modelling of the bone tissue, thermal properties and contact characteristics. To date it is possible to find disperse information concerning the mentioned aspects. The complexity of the cutting process in general requires finite element (FE) modelling in order to reproduce the factors influencing the output variables (mainly temperature, cutting forces and surface integrity). Among these factors the most important and complex one is the constitutive model of the bone. Even in the well-known case of metal or composite cutting operations, accurate modelling of mechanical behaviour of the workpiece is crucial for machining simulation, see for instance the recent works of the authors (Miguélez et al., 2013; Santiuste et al., 2011). These applications are good examples of isotropic (metal) and anisotropic (composite) workpieces.

Concerning the structure of bone, it is composed of two main tissues: the cortical bone in the outer surface region and trabecular bone in the inner regions and epiphysis of long bones. The cortical bone is made of hard, dense tissues and takes charge of the main compressive and bending loads. The trabecular bone is made of sparse, rod-like tissue to reduce structural mass (Kim et al., 2010).

Most works in the literature deal with the cutting operations of cortical bone since damage in this tissue is critical considering its structural responsibility, especially in long bones. Although a detailed revision of literature focusing on cortical bone cutting will be included in the following sections, a brief explanation of this tissue architecture is presented below.

Cortical bone is the first layer to be cut in any surgical operation. The microstructure of cortical bone (particularly at the diaphysis of long bones) is clearly anisotropic. In a micro-level (50–500 μm) it is possible to distinguish three relevant entities at this tissue level:

Recent osteons: cylinder shaped (in a first approximation) with diameter in the range 50–200 μm and length ranging from 3 to 5 mm. The osteons are formed by the continuous process of bone remodelling (Cowin, 2001; Taylor et al., 2007).

Interstitial matrix: mainly composed of rests of old osteons, with a higher mineral content than in recent

*Corresponding author.

E-mail address: mhmiguel@ing.uc3m.es (M. Henar Miguélez).

osteons. The interstitial matrix presents lower toughness than recent osteons (Taylor et al., 2007).

Cement line: a thin layer (about 1–5 μm, Nobakhti et al., 2014) surrounding the recent osteons. The cement line exhibits low toughness being a weak zone susceptible to crack propagation around the osteon (Nobakhti et al., 2014; Vercher et al., 2014; Li et al., 2013a; O'Brien et al., 2007).

Fig. 1 shows a scheme of cortical bone. The transverse isotropy of cortical bone is commonly assumed, i.e. the mechanical properties in directions 2 and 3 are considered identical but different to those in direction 1 (see Fig. 1).

Concerning the values of mechanical properties it is possible to find contributions of different authors in the literature, mainly dealing with strength analysis of bone, since cutting has been scarcely studied to date.

It is clear that the anisotropy of cortical bone exists, despite an isotropic approach in cutting bone modelling is often considered in the literature. This fact will be further discussed in the following sections.

The cancellous bone (also termed trabecular bone or spongy bone), is found inside the three dimensional boundary defined by the cortical bone. The cancellous bone makes up about 20% of the human skeleton, providing structural support and flexibility with low density. It is found in zones of bone that are not subjected to strong mechanical loading. The cancellous bone is light due to its porous structure, enclosing numerous large voids that give a honeycombed or spongy appearance. The bone matrix, or framework, is organized into a three-dimensional latticework of bone tissue, called trabeculae. The voids in between are often filled with marrow. Cancellous bone grows in response to an applied stress. Trabeculae develop along principal stress directions of the loaded bone (Jackson et al., 2005).

The main objective of this paper is to review the available information in the field of bone cutting modelling and to identify the best approach for the simulation of each process. The review concentrates mainly on finite element modelling, although other interesting contributions focusing on analytical or mechanistic models are included. In some cases experimental work is also referred since it gives light about the modelling process. Special attention is paid to the constitutive model of bone since a proper approach to the workpiece mechanical behaviour is crucial to reach accurate predictions. Constitutive modelling is also one of the main differences with metal or composite cutting simulation. In general, the know-how in these fields can be applied to bone cutting simulation, having into account the mechanical behaviour of bone. On the other hand fracture mechanics has been extensively developed in other fields and the knowledge generated can be applied to improve the modelling and understanding of cutting mechanisms in bone.

Most of the works in the literature focus on cutting operations of cortical bone. The present paper summarizes these works including also information concerning cancellous bone cutting when available.

The paper is structured in this introduction followed by the analysis of the modelling of the main bone cutting processes. The simplest machining process, orthogonal cutting is analysed in Section 2 of the paper. Despite its simplicity it is a good approximation to understand the complex problem of cutting. Drilling models are revised in Section 3. The works focusing on grinding and milling are reviewed in Section 4. In the following section other processes such as penetration are analysed. The main contributions obtained from the revised works are summarized in Table 1 that follows the same structure of the text (orthogonal cutting, drilling, grinding, milling and other processes). The aim of Table 1 is giving the reader a consistent overview of the literature, and also providing details such as the code used for simulations, the type of element and the value of friction coefficient, etc. These data are included when available in the original work. Since the information given in Table 1 is succinct, it is completed and commented in the different sections of the paper.

Some relationships between cutting and fracture mechanics are briefly described in Section 6. Finally, a short section summarizing information about cancellous bone cutting is included. Conclusions are presented in Section 8.

2. Orthogonal cutting

Both industrial and surgical machining processes are three-dimensional in essence due to the complex geometry of the cutting tool and its relative position to the workpiece. Despite the limitations of a two dimensional (2D) analysis this approach has been extensively used for simulation of machining for decades, in the field of metal and composite cutting. Simulation of orthogonal cutting has allowed the development of efficient models, with low computational cost, able to predict variables related to interface contact or surface integrity, see for instance recent works by the authors

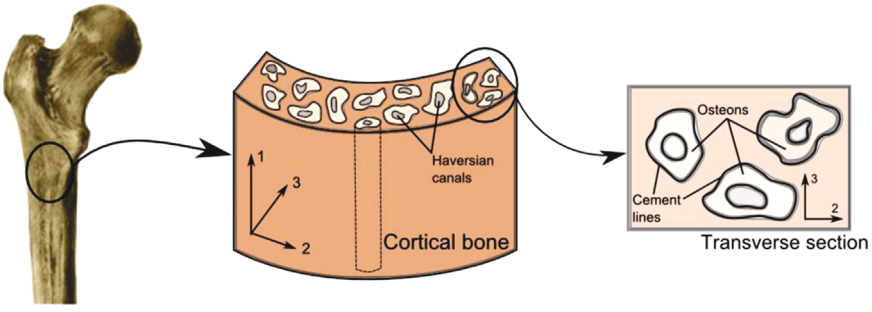

Fig. 1 – Simplified structure of cortical bone: recent osteons surrounded by cement line in an interstitial matrix composed of rests of old osteons.

Table 1: Summary of contributions of different authors to modelling of bone cutting.References cited in the table: Alam et al. (2009); Davidson and James (2000); Huiskes (1980); Alam et al. (2010); Reilly and Burstein (1974); Childs and Arola (2011); Keaveny et al. (2004); Santiuste et al. (2014); Rho et al. (1999); Singhranu et al. (1987); Stumme et al. (2003); Hage et al. (2013); Wang et al. (2014); Lughmani et al. (2013); Mitsuishi et al.(2005); Sezek et al. (2012); Tu et al. (2013); Tai et al. (2013); Wood (1971); Cezayirlioglu et al. (1985); Davy and Connolly (1982); Evans and Lissner (1957); McElhaney et al. (1970); Voor et al. (1997); Johnson and Rapoff (2007); Kasiri et al. (2010); Martin and Boardman (1993); Li et al. (2013b); Pithioux et al. (2002); Katz et al. (1984); Li et al. (2014).

<table>
<tr><th></th><th>Bone type</th><th>Material behavior model</th><th>Numerical analysis</th><th>Findings</th><th>Authors</th></tr>
<tr><td rowspan="3">Orthogonal cutting</td><td>Bovine, cortical</td><td>Equivalent heterogeneous material, with a Johnson-Cook model without influence of temperature:
$$\bar{\sigma}(\bar{\varepsilon}^p, \dot{\bar{\varepsilon}}^p) = [A + B(\bar{\varepsilon}^p)^n]\left[1 + C \ln\left(\frac{\dot{\bar{\varepsilon}}^p}{\dot{\bar{\varepsilon}}_0}\right)\right]$$
$$\Theta = \frac{T - T_0}{T_m - T_0}$$<table><tr><th colspan="2">Elastic properties</th><th colspan="2">Plastic properties (JC model)</th></tr><tr><td>Modulus (GPa)</td><td>20</td><td>A (MPa)</td><td>50</td></tr><tr><td>Friction coeff. (μ)</td><td>0.35</td><td>B (MPa)</td><td>101</td></tr><tr><td></td><td></td><td>C</td><td>0.03</td></tr><tr><td></td><td></td><td>n</td><td>0.08</td></tr></table></td><td>Model generated with MSC.Marc general FE code. The workpiece was discretized into four-node, isoparametric, arbitrary quadrilateral elements assuming plane strain conditions, and the cutting tool was modelled with isoparametric triangular elements. Remeshing was applied to avoid convergence issues associated with highly distorted elements.</td><td>The model predicted the cutting forces for various process parameters. The cutting force was affected by tool geometry and the depth, the material removal rate and extent of lubrication. The low depth of cut and cutting tool with the sharp edge reduces the cutting forces.</td><td>Alam et al. (2009)

Finite element analysis of forces of plane cutting of cortical bone</td></tr>
<tr><td>Bovine, cortical</td><td>The Johnson-Cook material model was utilized for the bone tissue. Johnson-Cook parameters were obtained from Alam et al. (2009).
Thermal properties were obtained from Davidson and James (2000) and Huiskes (1980).<table><tr><th colspan="2">Thermal properties</th></tr><tr><td>Thermal conductivity (W/mK)</td><td>0.56</td></tr><tr><td>Heat capacity (J/m^{3}K)</td><td>$2.86 \cdot 10^6$</td></tr></table></td><td>Model generated with MSC.Marc general FE code. A thermomechanically coupled 2D model of bone cutting was developed to simulate temperatures during the high-speed cutting process. The workpiece was modelled with four-node, isoparametric, arbitrary quadrilateral elements and assuming plane strain conditions. Remeshing was applied to avoid high element distorsion.</td><td>The model allowed the study of chip formation and predictions of temperature rise. High cutting speeds were critical in inducing thermal necrosis of bone tissue. The presence of adequate cooling conditions can reduce the risk of inflicting thermal injury to the bone tissue. The temperature rise and necrosis penetration were affected by cutting speed, depth of cut and bone thermal properties.</td><td>Alam et al. (2010)

Thermal analysis of orthogonal cutting of cortical bone using finite element simulations</td></tr>
<tr><td>Human, bovine, cortical.</td><td>A range of pressure-dependent yield stress models, with strain-path dependent failure laws was created and used to evaluate the chip formation. Material with flow stress dependence on strain and strain-rate, temperature dependence was ignored:
$$\bar{\sigma}(\bar{\varepsilon}^p, \dot{\bar{\varepsilon}}^p, T) = \sigma_0\left(1 + \frac{\bar{\varepsilon}^p}{\bar{\varepsilon}_0{}^p}\right)^{\frac{1}{n}}(1 + \dot{\bar{\varepsilon}}^p)^{\frac{1}{m}}$$Properties obtained from the work of Reilly and Burstein (1974).<table><tr><th>σ_0 (MPa)</th><th>$\bar{\varepsilon}_0^p$</th><th>n</th><th>m</th><th>Friction coeff. (μ)</th></tr><tr><td>200</td><td>0.009</td><td>0.022</td><td>0.02</td><td>0.2 and 0.1</td></tr></table></td><td>The model was developed with the commercial metal machining FE software AdvantEdge-2DTM.
There is no element or node elimination, so a crack does not open up, but chip fragmentation may occur as a result of the action of remeshing routines. No element type specified.</td><td>The ratio of thrust force to cutting force is sensitive to the cutting edge profile. The failure of the carbide edges in machining of bone was explained arguing that the tensile stresses are concentrated at the contact of the cutting edge with the osteons within the bone matrix.</td><td>Childs and Arola (2011)

Machining of cortical bone: simulations of chip formation mechanics using metal machining models</td></tr>
</table>

<table>
<tr>
<td rowspan="2">Orthogonal cutting</td>
<td>Bovine, cortical</td>
<td>Isotropic model with rate dependent (JC), anisotropic model (influence of osteon orientation): as a fiber reinforced composite material, elastic behavior up to failure predicted with Hou model, implemented through a VUMAT. Isotropic material properties and JC parameters were obtained from the work of Alam et al (2009).
Anisotropic properties of cortical bone, obtained from Keaveny et al. (2004).
<table>
<tr><th colspan="2">Elastic and thermal properties</th><th colspan="3">Ultimate stress</th></tr>
<tr><td>Longitudinal modulus E_1 (GPa)</td><td>17.90</td><td colspan="2">Longitudinal (MPa)</td><td>Shear (MPa)</td></tr>
<tr><td>Transverse modulus E_2 (GPa)</td><td>10.1</td><td>Tension, X_T</td><td>135</td><td>65</td></tr>
<tr><td>Shear modulus G_{12} (GPa)</td><td>3.3</td><td>Compression, X_c</td><td>202</td><td></td></tr>
<tr><td>Thermal Conductivity (W/m K)</td><td>0.56</td><td colspan="3">Transverse (MPa)</td></tr>
<tr><td>Specific heat (J/kg K)</td><td>1260</td><td>Tension, X_T</td><td>53</td><td></td></tr>
<tr><td>Friction coeff. (μ)</td><td>0.35</td><td>Compression, X_c</td><td>131</td><td></td></tr>
</table></td>
<td>2D: plane strain, Abaqus/Explicit, based on a Lagrangian formulation, linear quadrilateral elements of type CPE4RT (plane strain, quadrilateral, linearly interpolated, and thermally coupled elements with reduced integration and automatic hourglass control).
3D: dynamic explicit analysis including non-linearity and large deformation options. Longitudinal, across and transverse osteon orientation.</td>
<td>The influence of the osteon orientation on the cutting force is important, the across and transverse orientations lead to the maximum levels of force. The across and transverse orientation showed lower values of temperature than 47ºC, corresponding with osteonecrosis.</td>
<td>Santiuste et al. (2014)

The influence of anisotropy in numerical modelling of orthogonal cutting of cortical bone</td>
</tr>
<tr>
<td>Bovine, cortical</td>
<td>Cortical bone as an heterogeneous material. The flow stress of the osteon and lamellae matrix regions were assumed to behave according to a JC material model (whose parameters were obtained from Alam et al. (2009)).
Properties obtained from: Rho et al. (1999), Singhranu et al (1987), Stumme et al (2003) and Alam et al. (2009).
<table>
<tr><th></th><th>Osteons</th><th>Lamellae matrix</th></tr>
<tr><td>Young’s modulus (GPa)</td><td>20.8</td><td>26.3</td></tr>
<tr><td>Hardness (GPa)</td><td>0.65</td><td>0.79</td></tr>
<tr><td>Poisson’s ratio</td><td>0.3</td><td>0.3</td></tr>
<tr><td>Thermal expansion (mm/°C)</td><td>2.75e-5</td><td>2.75e-5</td></tr>
<tr><td>Emissivity</td><td>1</td><td>1</td></tr>
<tr><td>Thermal conduc. (N/sec°C)</td><td>0.58</td><td>0.58</td></tr>
<tr><td>Heat capacity (N/mm^2°C)</td><td>2.86e+12</td><td>2.86e+12</td></tr>
<tr><td></td><td>Frict. coeff. (μ)</td><td>0.35</td></tr>
</table></td>
<td>Model generated with DEFORM. Tetrahedral elements were used to mesh the tool and the bone, with a minimum element size of 0.14 μm. Active re-meshing was considered with a relative interference ratio of 0.7 and a maximum stroke increment of 1 μm to ensure proper interaction between the tool and work.</td>
<td>The feed force and tangential cutting force components agreed favorably with experimental results. Although at the end the values are comparable, the start of the predicted force development in the simulations is less steep than in experimental results.</td>
<td>Hage et al. (2013)

Micro-FEM orthogonal cutting model for bone using microscope images enhanced via artificial intelligence</td>
</tr>
</table>

<table>
<tr><td rowspan="3">Drilling</td><td>Bovine, cortical</td><td>Since this is a 2D thermal analysis, only thermal properties of cortical bone were employed.

<table><tr><th>Density (kg/m^3)</th><th>Conductivity(W/m°C)</th><th>Specific heat (J/kg °C)</th></tr><tr><td>1700</td><td>0.38</td><td>1260</td></tr></table></td><td>A 2D finite element model was generated with the software package GAMBIT and used to simulate the cutting heat conduction in vibrational and conventional drilling. The screw thread was ignored in the drill bit. In order to consider the impact of air flow on the thermal conduction, an air layer 0.1 mm thick was constructed between the drill bit and the bone. The model was constructed using triangles.</td><td>Vibrational drilling could significantly reduce the cutting heat in drilling of cortical bone ($P < 0.05$). It is also found that with the increase of vibration frequency and amplitude, there is a downward trend of cutting temperature of bone. However, the simulation showed that the effect of vibration frequency (less than 100 Hz) on the cutting heat conduction was not particularly obvious.</td><td>Wang et al. (2014)

Experimental investigations and finite element simulation of cutting heat in vibrational and conventional drilling of cortical bone</td></tr>
<tr><td>Human, cortical</td><td>Cortical bone was modelled as a rate dependent transversely isotropic material, using the elastic-plastic law for the material constitutive model. The high strain rate data were obtained by using Split Hopkinson Pressure Bar (SHPB) experiments. A dynamic failure criterion is applied to control the element removal when the plastic strain reaches a specific value.

<table><tr><td>Density (kg/m^3)</td><td>2000</td></tr><tr><td>Young’s modulus longitudinal (GPa)</td><td>20</td></tr><tr><td>Young’s modulus transverse (GPa)</td><td>18</td></tr><tr><td>Strain at failure %</td><td>5</td></tr><tr><td>Friction coefficient (μ)</td><td>0.7</td></tr></table></td><td>A three dimensional (3D) Lagrangian FE model of drilling of cortical was developed in Abaqus/Explicit. A refined mesh with a minimum size of 5 μm was used at and in the immediate vicinity of the volume to be drilled. The cortical bone was modelled using 8-node, 3D brick elements. Contact between the twist drill and the cortical bone was defined by the general contact algorithm which generated the contact forces based on the penalty-enforced contact method.</td><td>The FE model predicted the drilling thrust force and torque with reasonable accuracy when compared to experimental results. It was observed that the thrust force and torque increased with an increase in the feed rate and spindle speed. Thrust force and torque may be reduced by using the low feed with a high spindle speed.</td><td>Lughmani et al. (2013)

Finite element modelling and experimentation of bone drilling forces</td></tr>
<tr><td>Calf, cortical</td><td>Bone modelled as a hollow cylinder and obeying to an homogeneous and isotropic material, elastic behavior. Friction coefficient was not studied in the work.
Properties obtained from Mitsuishi et al. (2005).

<table><tr><td>Specific heat (cal/g °C)</td><td>0.27 ± 0.001</td></tr><tr><td>Thermal conductivity (cal/cms °C)</td><td>100</td></tr><tr><td>Tensile strength (MPa)</td><td>48</td></tr><tr><td>Elongation</td><td>0.9%</td></tr><tr><td>Elasticity modulus (GPa)</td><td>10.2</td></tr><tr><td>Poisson’s ratio</td><td>0.36</td></tr><tr><td>Shear modulus (GPa)</td><td>3.6</td></tr></table></td><td>Model developed using the backing MSC Software. Element size was taken as 0.01 mm, with triangles. Remeshing was used in order to prevent the mesh impairment due to bone sawdust formation.</td><td>Optimum drill force was 140 N, speed (370 rpm) and feed-rate (70mm/min).
Applied drill force increased as bone density increased, temperature increased 10% with a 12% increase in bone density.
Temperature decreased by 20% for every mm of distance away from the drill site. Transient temperature change was detected to be 132ºC/s maximum.</td><td>Sezek et al. (2012)

Influence of drill parameters on bone temperature and necrosis: A FEM modelling and in vitro experiments</td></tr>
</table>

<table>
<tr>
<td>Drilling</td>
<td>Pig femur cortical and trabecular</td>
<td>Bone modelled with elastic behavior, with yield strength. The criterion used to delete an element is based on the value of effective plastic displacement, which was set as 0.1 mm.
Properties were provided by Sawbones.
<table>
<tr><th></th><th>Cortical bone (analogue)</th><th>Cancellous bone (analogue)</th></tr>
<tr><td>Young’s modulus (GPa)</td><td>16.7</td><td>1</td></tr>
<tr><td>Density (kg/m^3)</td><td>1640</td><td>640</td></tr>
<tr><td>Yield strength (MPa)</td><td>105</td><td>19</td></tr>
<tr><td>Tensile strength (MPa)</td><td>106</td><td>19.1</td></tr>
<tr><td>Specific heat (J·kg^{-1}·°C^{-1})</td><td>1640</td><td>1477</td></tr>
<tr><td>Poisson’s ratio</td><td>0.3</td><td>0.055</td></tr>
<tr><td>Conductivity (W/K·m)</td><td>0.452</td><td>0.087</td></tr>
<tr><td></td><td>Friction coeff. (μ)</td><td>0.3</td></tr>
</table></td>
<td>This study was developed with Abaqus/Explicit, and utilized a three-dimensional elastic-plastic temperature-displacement coupled FEM with dynamic failure criterion applied to control the element removal during the drilling operation. The friction behavior between the drill bit and bone is assumed to be governed by Coulomb’s friction law. The mesh is constructed using eight-node three-dimensional brick elements.</td>
<td>The peak temperature increases more than 27 °C within a distance of 0-0.5 mm from the drilled hole. The peak bone temperature and the size of the thermally affected zone increase with increasing drilling speed. The peak temperature difference obtained from the proposed FE model and the experiment is less than 3 °C. The sizes of the thermally affected zone obtained from drilling speeds at n = 600, 800, and 1200 rpm are 0.35, 0.7, and 1.38 mm, respectively.</td>
<td>Tu et al. (2013)

Finite element simulations of bone temperature rise during bone drilling based on a bone analogue</td>
</tr>
<tr>
<td>Grinding</td>
<td>Bovine, cortical femur</td>
<td>No thermal properties specified. The model determines heat generation based on its linear correlation to the motor electrical power. To quantify the electrical power, a pulse-width-modulation (PWM) signal, was used. For the heat generation, inverse heat transfer method (IHTM) was applied.</td>
<td>The percentage of heat flowing to the bone is defined as heat conversion ratio □.
Moving heat source is applied on the spherical interface between bone and tool in the form of surface heat flux.
The elements are removed sequentially toward the feeding direction to expose another round patterns for the next time step. No element type specified.</td>
<td>Experimental results demonstrated the linear correlation between the motor electrical power and heat generation. The FEA thermal model yielded accurate temperature prediction. The entire temperature monitoring method could be converted into a real-time temperature feedback. This way can reduce the risk of thermal injury.</td>
<td>Tai et al. (2013)

Neurosurgical bone grinding temperature monitoring</td>
</tr>
<tr>
<td>Other processes</td>
<td>Human, cortical

Penetration</td>
<td>Elastic isotropy was used to represent human skull cortical bone. Von Mises’ yield criterion was used and the yield and plasticity characteristics were input according to a bilinear elastic-plastic material behavior assumption.
Properties obtained from: Reilly and Burstein (1975), Wood (1971), Cezayirlioglu et al. (1985), Davy and Connolly (1982), Evans and Lissner (1957), McElhaney et al. (1970).
<table>
<tr><td>Young’s modulus (GPa)</td><td>15</td></tr>
<tr><td>Poisson’s ratio</td><td>0.35</td></tr>
<tr><td>Yield stress (MPa)</td><td>180</td></tr>
<tr><td>Strain hardening slope (MPa)</td><td>1000</td></tr>
<tr><td>Ultimate compressive stress (MPa)</td><td>220</td></tr>
<tr><td>Friction coeff. (μ)</td><td>0.1</td></tr>
</table></td>
<td>An axisymmetric model of halo pin insertion was developed with PATRAN. The pin was modeled as a separate rigid body. The bone portion of the model employed eight-noded biquadratic elements. The contact analysis was performed as rigid body contact between the pin (rigid body) and the bone disk (deforming body). Variation of the Coulomb friction coefficient from 0.0001 to 0.4 had negligible effects in the model. The solutions to the analyses were achieved through an iterative process using the Newton indirect method.</td>
<td>The pin penetration depth and the shape of the profile of the hole formed in the skull bone were similar between model and mechanical tests, including the raised rim of bone around the periphery of the hole. No true material failure criteria were modelled, but because the loading was primarily compressive, using full plasticity at the ultimate stress level was considered appropriate.</td>
<td>Voor et al (1997)

Stress analysis of halo pin insertion by non-linear finite element modelling</td>
</tr>
</table>

<table>
<tr>
<td rowspan="2">Other processes</td>
<td>Bovine, cortical

Indentation</td>
<td>Bone was modeled as an isotropic bilinear material with von Mises plasticity. The tangent modulus and yield stress were varied until agreement was obtained with the experimental force-displacement data.
Properties obtained from Johnson and Rapoff (2007).
<table>
<tr><th></th><th>Longitudinal</th><th>Transverse</th><th>Tangential</th></tr>
<tr><td>Young’s modulus (GPa)</td><td>18</td><td>10</td><td>8.5</td></tr>
</table>
</td>
<td>The model was built using ANSYS, no element type specified. The fracture of bovine bone under indentation was measured experimentally and predicted using the theory of critical distances (TCDs). Two-dimensional plane strain models were used, with symmetry conditions.</td>
<td>Fracture force is affected by the bone orientation and blade radius. The TCD, in combination with the Coulomb–Mohr fracture criterion, was able to accurately predict the experimental fracture forces. Crack growth is easier in the tangential direction than in the longitudinal. Major cracks grow in the weakest possible structural direction.</td>
<td>Kasiri et al. (2010)

Wedge Indentation Fracture of Cortical Bone: Experimental Data and Predictions</td>
</tr>
<tr>
<td>Bovine femur, cortical

Penetration</td>
<td>Transversely isotropic elastic-plastic material incorporating the Hill’s anisotropic yield criteria and progressive degradation. The onset of damage was assumed when a failure strain of 2% was reached. Damage evolution process was governed by an energy-based criterion.
Properties obtained from: Martin and Boardman (1993), Li et al. (2013b), Pithioux et al (2002), Katz et al. (1984), Reilly and Burstein (1975).
<table>
<tr><th></th><th>Anterior</th><th>Posterior</th><th>Medial</th><th>Lateral</th></tr>
<tr><td>Density (kg/m^3)</td><td>2</td><td>2</td><td>2</td><td>2</td></tr>
<tr><td>E_1 (GPa)</td><td>23.2</td><td>19.3</td><td>21.1</td><td>15.1</td></tr>
<tr><td>E_2, E_3 (GPa)</td><td>13.2</td><td>9.9</td><td>14.7</td><td>11.2</td></tr>
<tr><td>ν_{12}, ν_{13}</td><td>0.27</td><td>0.27</td><td>0.27</td><td>0.27</td></tr>
<tr><td>ν_{23}</td><td>0.39</td><td>0.39</td><td>0.39</td><td>0.39</td></tr>
<tr><td>G_{12}, G_{13} (GPa)</td><td>6.1</td><td>6.1</td><td>6.1</td><td>6.1</td></tr>
<tr><td>ε_{y1} (%)</td><td>1</td><td>1</td><td>1</td><td>1</td></tr>
<tr><td>ε_{f1}, ε_{f2} (%)</td><td>2</td><td>2</td><td>2</td><td>2</td></tr>
<tr><td>J_{IC1} (N/m)</td><td>1653</td><td>1534</td><td>1868</td><td>2664</td></tr>
<tr><td>J_{IC2} (N/m)</td><td>4087</td><td>3029</td><td>4765</td><td>4296</td></tr>
</table>
<table>
<tr><td>Friction coeff. (μ)</td><td>0.3</td></tr>
</table>
Hill parameters
<table>
<tr><th>F</th><th>G</th><th>H</th><th>L</th><th>M</th><th>N</th></tr>
<tr><td>2.8</td><td>0.5</td><td>0.5</td><td>3</td><td>6</td><td>6</td></tr>
</table>
</td>
<td>A new 3D finite-element modelling approach (encompassing both conventional and SPH elements) was created with Abaqus/Explicit. In the SPH domain, the smoothing length was 2.2 times of the characteristic length of the associated particle volume. A plane strain condition was assumed throughout the thickness of the specimen. Particle elements, (PC3D in Abaqus) were implemented in the middle section of the specimen and continuum brick elements (C3D8R in Abaqus) in remaining sections. The cutting tool was modelled as an analytical rigid body and measured using a 3D scanning optical microscope.</td>
<td>An anisotropic behavior of the penetration process was detected: high for direction perpendicular to osteons and low for that parallel to osteons. However, there is no substantial difference with the tool parallel to osteons, between longitudinal and transverse orientation. The obtained results in the numerical model agreed well with the experimental findings, and the model successfully manifested the non-uniformity and anisotropy of deformation and damage processes.</td>
<td>Li et al. (2014)

Penetration of cutting tool into cortical bone: Experimental and numerical investigation of anisotropic mechanical behavior</td>
</tr>
</table>

in the field of metal and composite cutting (Molinari et al., 2012; Soldani et al., 2011).

The analysis of orthogonal cutting of bone has enabled the investigation of cutting characteristics such as forces, chip morphology and surface integrity since the 70's. Jacobs et al. (1974) studied the influence of feed and rake angle on cutting forces and the chip morphology. Wiggins and Malkin (1978) increased the range of parameters of this study. They proposed a fracture based chip formation model and defined a linear correlation between specific energy and surface to volume ratio. The influence of cutting speed and rake angle on cutting forces was studied by Krause (1987) concluding that the cutting forces and specific cutting energy decreased when the cutting speed was increased. These early studies gave an experimental approach to the problem. Further developments have been included in analytical and finite element models for prediction of cutting forces and temperature.

Jacobs et al. (1974) demonstrated the low applicability of Merchant's model (developed for metal cutting, Merchant, 1945a, 1945b) for prediction of cutting forces with respect to cutting direction relative to the dominant osteon direction. In a recent work, Sui et al. (2013) developed an analysis of variance (ANOVA) and regression analysis to study the effects of cutting conditions on cutting and thrust forces based on a full factorial design. The suitability of Merchant's analysis for calculating cutting force with respect to rake angle and feed was evaluated through comparison with experiments. The trend of cutting forces calculated by Merchant's theory is similar to that observed with experiments, showing a maximum relative error of cutting force of about 34%.

Many efforts have also been developed in the field of finite element simulation. The models are classified in different subsections based on the approach to constitutive modelling of the bone, either assuming isotropic behaviour or accounting for anisotropy. Also a brief summary of micro-scale modelling is included.

2.1. *FE assuming isotropic behaviour*

Despite the anisotropic structure of bone, the assumption of isotropic behaviour has been commonly adopted in the literature for simulation of cutting. An isotropic approach in bone cutting modelling was presented in Alam et al. (2009). These authors carried out an experimental and numerical study focused on orthogonal cutting of bone. A two dimensional modelling of the process assuming elastic–viscoplastic behaviour of the bone for cutting forces and temperature prediction was presented. The mechanical response is represented by the Johnson–Cook law (without thermal softening). The Johnson–Cook model has been widely used for the simulation of metal cutting (see for instance, the recent works by the authors, Molinari et al., 2012).

This model assumes von Mises J2 plasticity criteria based on a Johnson–Cook hardening law. Von Mises yield surface is defined by tension/compression symmetry. The Johnson–Cook hardening law is frequently applied to analyse the dynamic behaviour of metal alloys. This hardening law is generally pre-implemented in FE codes, including ABAQUS/Explicit. The Johnson–Cook model is defined by Eq. (1). The first term in brackets defines the strain hardening $\bar{\varepsilon}^p$, the second the strain rate sensitivity, $\dot{\bar{\varepsilon}}^p$ via the constant C and the third one is related to thermal softening.

$$\bar{\sigma}\left(\bar{\varepsilon}^p, \dot{\bar{\varepsilon}}^p, T\right) = \left[A + B(\bar{\varepsilon}^p)^n\right]\left[1 + C \ln \frac{\dot{\bar{\varepsilon}}^p}{\dot{\bar{\varepsilon}}_0}\right]\left[1 - \Theta^m\right] \tag{1}$$

$$\Theta = \frac{T - T_0}{T_m - T_0} \tag{2}$$

where A and B are the material constants, n is the strain hardening exponent, m is the temperature sensitivity, T_0 is the initial temperature and T_m is the melting temperature.

Through experimental characterization of bone, Keaveny et al. (2004) obtained its strain rate sensitivity at high strain rates. Alam et al. (2009) proposed to neglect the influence of temperature on the yield stress due to small temperature changes leading to negligible thermal softening. In this sense, Eq. (1) leads to the following equation:

$$\bar{\sigma}\left(\bar{\varepsilon}^p, \dot{\bar{\varepsilon}}^p\right) = \left[A + B(\bar{\varepsilon}^p)^n\right]\left[1 + C \ln\left(\frac{\dot{\bar{\varepsilon}}^p}{\dot{\bar{\varepsilon}}_0}\right)\right] \tag{3}$$

These constants are reported in Table 1 summarizing details of constitutive parameters for different cutting models.

The same approach to the mechanical behaviour of bone given in Alam et al. (2009) was used in Alam et al. (2010). In the latter, a two dimensional model was applied to predict temperatures reached during bone drilling. Although the process is simplified considering orthogonal cutting and assuming an equivalency to cutting with the external side of the drill edge, reasonable accuracy is observed regarding the temperature prediction.

The estimation of apparent toughness of bone from machining tests performed by Wiggins and Malkin (1978) yielded the same order of magnitude as fiber reinforced plastic, being larger than cast iron. This behaviour supports the use of a plastic strain accumulation damage law, coupled with a plasticity analysis, for modelling chip formation in bone machining.

Childs and Arola (2011) assessed the applicability of a metal machining finite element model to predict chip formation and forces in bone cutting. The uncoupled continuum model is based on two different concepts: an elasto-viscoplastic material model and a fracture criterion.

The isotropic hardening law included the effect of strain rate and thermal softening:

$$\bar{\sigma}(\bar{\varepsilon}^p, \dot{\bar{\varepsilon}}^p, T) = \sigma_0\left(1 + \frac{\bar{\varepsilon}^p}{\bar{\varepsilon}_0{}^p}\right)^{\frac{1}{n}}\left(1 + \dot{\bar{\varepsilon}}^p\right)^{\frac{1}{m}}\Theta(T) \tag{4}$$

Thermal softening was ignored as in Alam et al. (2009) because of the small temperature increments induced in bone cutting. Thus, Eq. (4) leads to the following equation:

$$\bar{\sigma}\left(\bar{\varepsilon}^p, \dot{\bar{\varepsilon}}^p, T\right) = \sigma_0\left(1 + \frac{\bar{\varepsilon}^p}{\bar{\varepsilon}_0{}^p}\right)^{\frac{1}{n}}\left(1 + \dot{\bar{\varepsilon}}^p\right)^{\frac{1}{m}} \tag{5}$$

Being $\bar{\sigma}$ the effective elastic limit, $\bar{\varepsilon}^p$ the equivalent plastic strain, $\dot{\bar{\varepsilon}}^p$ the equivalent plastic strain rate and, T the temperature. σ_0, $\bar{\varepsilon}_0^p$, n and m are the constants provided in Table 1. These values were stated according to experimental observations in Reilly and Burstein (1974) who found that the flow

stress varies from 200 to 270 MPa when the strain increases from 0 to 1.0 and the strain-rate increases from 1 to 10^4 s^{-1}.

2.2. *FE assuming anisotropic behaviour*

Although isotropic models have been assumed for bone behaviour modelling due to their simplicity, early experiments in the 70's showed the influence of osteon orientation in the mechanical response of bone. Reilly and Burstein (1974) obtained low strain-rate strengths for human and bovine cortical bone (values are summarized in Table 2). In compressive conditions, strengths of bovine bone are 50% larger than human bone. When the principal stress axis is coincident with the osteon direction, strengths are 50% greater than when the principal stress direction is perpendicular to the osteon direction. Strengths are lower in tension, especially when loading orthogonal to the osteon direction, however the difference between bovine and human bone is lower.

Not only strength changes with the stress direction, but also the elastic modulus and yield stress vary with the load orientation (Keaveny et al., 2004).

Yeager et al. (2008) examined the influence of osteon orientation (i.e. taking into account the bone anisotropy) and cutting conditions on the surface roughness and integrity resulting from orthogonal machining. They performed a factorial evaluation of the cutting direction and other conditions, concluding that the largest range of cutting forces and surface roughness occurred when machining in the transverse direction (i.e. the machined surface is perpendicular to the osteon direction). This is consistent with the results of Jacobs et al. (1974) and Wiggins and Malkins (1978).

Numerous other studies corroborate the anisotropic behaviour of bone, see some examples in Nordin and Frankel (2001), O'Mahony et al. (2001), and Vercher et al. (2014).

The bone anisotropy also influences chip generation mechanisms depending on the osteon orientation (see Fig. 2 showing the different orientations considered in orthogonal cutting). Sugita et al. (2009a) performed orthogonal cutting tests in cortical bone, assuming that cortical bone can be considered a one-directional, continuous fiber reinforced type of composite material. Experimental evidence corroborates this assumption as can be observed in Fig. 2.

In a recent work by the authors similar prediction of chip morphology has been achieved based on a numerical analysis (Santiuste et al., 2014). Orthogonal cutting of cortical bone was analysed using finite elements. The bone was modelled as an anisotropic material using a similar approach to that

Table 2 – Low strain-rate compressive and tensile strengths of bovine and human cortical bone (Reilly and Burstein, 1974).

Bone source	Compressive strength (MPa) // Osteon direction	⊥ Osteon direction	Tensile strength (MPa) // Osteon direction	⊥ Osteon direction
Bovine	220–280	150–190	110–170	30–60
Human	130–190	100–130	120–150	~50

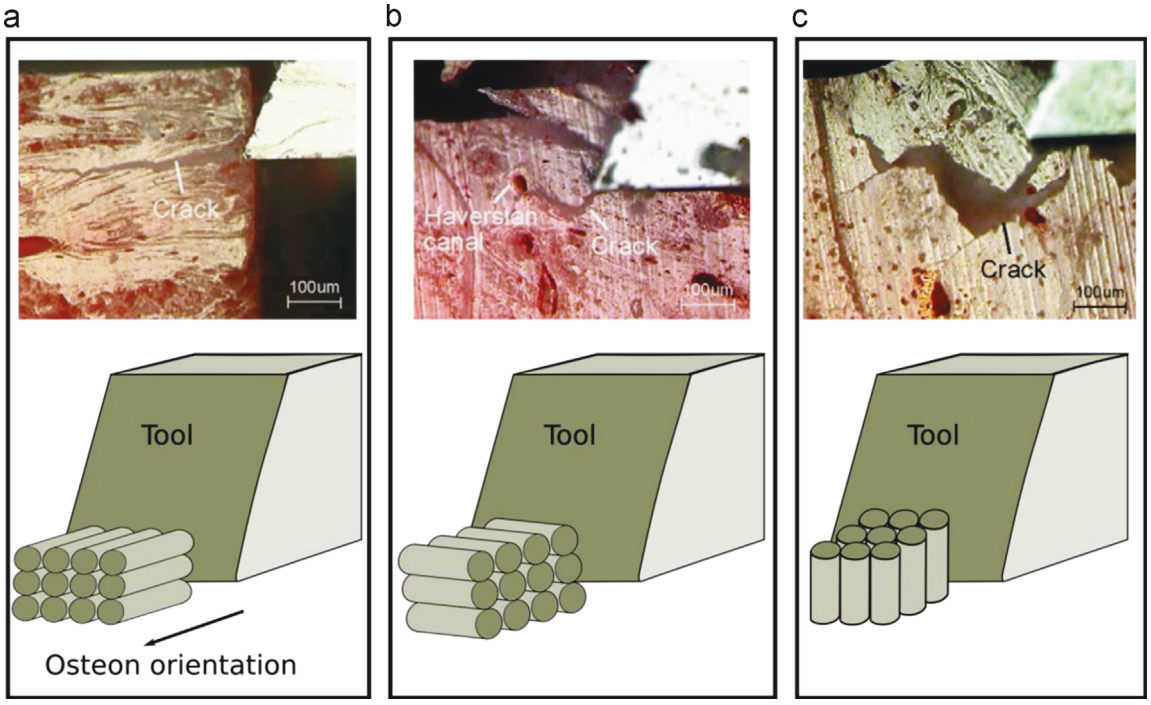

Fig. 2 – Scheme of osteon orientation considered in orthogonal cutting and experiments performed by Sugita et al. (2009a) showing crack propagation during orthogonal cutting of cortical bone depending on cutting direction: (a) longitudinal; (b) across; and (c) transverse.

used for long fiber reinforced composites. In this case the osteons played the role of fibers reinforcing the interstitial matrix. The model commonly used in the literature for the simulation of composite cutting was validated through the comparison with experimental results provided in Alam et al. (2009), (2010).

Since the stiffness and strength are the highest in the longitudinal direction (when the osteons direction coincides with the loading direction), the assumption of mechanically isotropic bone tissue is a strong simplification of the problem. The cortical bone can be properly modelled as a rate dependent transversely isotropic material (Reilly and Burstein, 1975; Yoon and Katz, 1976) thus this tissue can be considered analogous to a fiber reinforced composite material as has been demonstrated in different contributions in the literature; see for instance Guo et al. (1998), Hogan (1992), Katz et al. (1984), and Bigley et al. (2006).

Based on this analogy, the osteon behaves as the fiber with the interstitial bone consisting of old osteon fragments acting as the matrix. Different studies on fracture mechanics of cortical bone have demonstrated similarities to fracture mechanics in composite materials, see for instance Guo et al. (1998), Alto and Pope (1979), Bell et al. (1999), Martin et al. (1996), Moyle et al. (1978), and Giner et al. (2014).

In Santiuste et al. (2014), the anisotropic cortical bone was modelled assuming an elastic behaviour up to failure. Failure was predicted with the Hou model, see Table 3 summarizing failure modes proposed in Hou et al. (2000).

Hou's approach, commonly used in composite mechanics, proposes the same formulation under tensile and compressive loading for fiber failure criterion, including longitudinal shear stresses σ_{12} and σ_{13}. The transverse shear stress σ_{23} was included for matrix cracking criterion. Parameters in Table 3 are as follows: σ_{11}, σ_{22}, and σ_{33}, are the stresses in longitudinal, transverse and through-the-thickness direction respectively; σ_{12}, σ_{23}, and σ_{13}, are the shear stresses; X_T and X_C are the tensile and compressive strengths in longitudinal direction; Y_T and Y_C are the tensile and compressive strengths in the transverse direction; S_L is the longitudinal shear strength; S_T is the transverse shear strength. Failure occurs when any damage variable (d_{ij}) reaches the value 1.

Hou's formulation was implemented into a three dimensional analysis through a VUMAT user subroutine, developed to model fiber reinforced composites, including a procedure to degrade material properties. In Santiuste et al. (2014) it was applied to the simulation of cortical bone behaviour. Under a given load, the stresses at each integration point were computed in the user subroutine. Then, each failure criterion was calculated as a function of stresses and, if any failure mode was reached, the material properties at that point were degraded according to the failure mode. When a failure criterion was verified within any element, stresses are reduced, reproducing the degraded behaviour according to the failure mode.

Table 3 – Hou damage criteria: failure modes for fiber and matrix.

Failure mode	*Hou formulation*
Fiber tension	$d_{ft}^2 = \left(\frac{\sigma_{11}}{X_T}\right)^2 + \left(\frac{\sigma_{12}^2+\sigma_{13}^2}{S_L^2}\right)$
Fiber compression	$d_{fc}^2 = \left(\frac{\sigma_{11}}{X_C}\right)^2 + \left(\frac{\sigma_{12}^2+\sigma_{13}^2}{S_L^2}\right)$
Matrix cracking	$d_{mt}^2 = \left(\frac{\sigma_{22}}{Y_T}\right)^2 + \left(\frac{\sigma_{12}}{S_L}\right)^2 + \left(\frac{\sigma_{23}}{S_T}\right)^2$
Matrix crushing	$d_{mc}^2 = \frac{1}{4}\left(\frac{-\sigma_{22}}{S_T}\right)^2 + \left(\frac{Y_c\,\sigma_{22}}{4S_T^2}\right) - \left(\frac{\sigma_{22}}{Y_C}\right) + \left(\frac{\sigma_{12}}{S_L}\right)^2$

The reduction of elastic properties could lead to distorted elements involving numerical problems, thus the model required the use of an element erosion criterion. Stresses on a damaged element drop to values close to zero while large deformations appear. These elements do not contribute to the strength or the stiffness of the plate, but they can cause lack of convergence during simulation and instability problems.

The material parameters for Hou's model were obtained from the work of Keaveny et al. (2004) and they are included in Table 1. These values are homogenized properties to be input in the numerical model. Properties in direction 1 and 2 are in the same order. This is a strong difference when comparing with structural composites such as CFRP, which exhibit longitudinal stiffness two orders of magnitude higher than transverse stiffness. Concerning the strength properties, longitudinal values are higher both in tension and compression. Osteons are mainly aligned with the axis of the diaphysis of the long bone (although obviously some misalignment is found in the actual tissue). The natural design imposes higher strength in the axis direction of the long bone than in the transverse direction in order to bear the usual loading state. On the other hand, compression behaviour is enhanced since the compressive loading in long bones is larger than tensile.

As a result from the analyses considering model anisotropy, it was concluded that the influence of the osteon orientation on the cutting force is significant. The orientations across and transverse to the cutting speed direction, lead to the maximum levels of force, thus confirming the behaviour observed experimentally in the literature.

The thermally affected zone also depends on the osteon orientation. The level of 47 °C corresponding to osteonecrosis was reached for the longitudinal orientation, however the across and transverse orientation showed lower values of temperature.

The chip morphology strongly depends on the osteon orientation, changing from continuous chip for longitudinal orientation, to serrated chip for the transverse orientation. The anisotropic approach gave realistic chip morphology similar to that observed in experiments in Fig. 2 as it is shown in Fig. 3.

2.3. *Micro-scale modelling*

Modelling at the micro-scale seems to be an adequate approach for bone cutting simulation. Hage and Hamade (2013) analysed orthogonal cutting of cortical bone from a micro-structural perspective (Fig. 4). The micro-structure of the bone was identified from an optical image taken from bovine femur cortical bone slice. The bone images at the microstructure level were enhanced and the micro-constituents of the bone were segregated as separate images. The flow stresses of the osteon and lamellae matrix regions were assumed to behave according to a Johnson–Cook

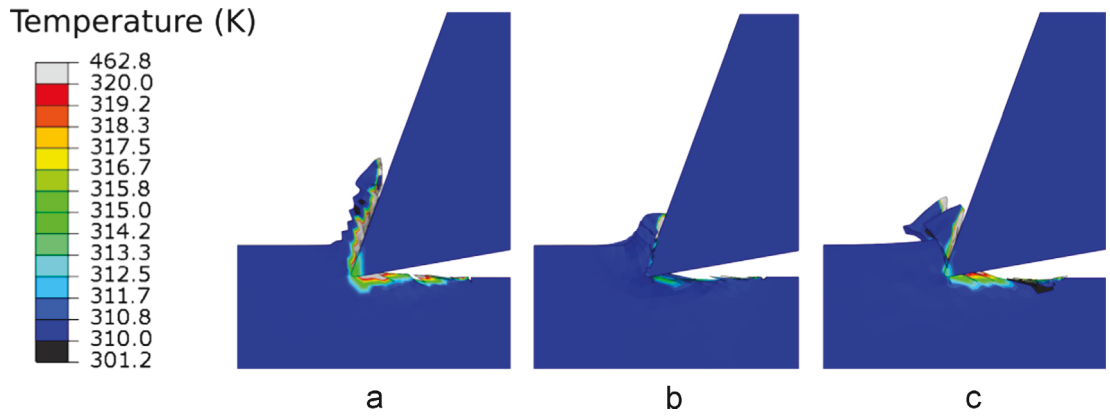

Fig. 3 – Temperature contours and chip morphology obtained for different. (a) Longitudinal; (b) transverse; and (c) across (Santiuste et al., 2014).

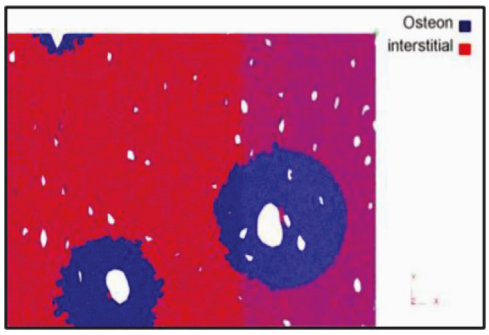

Fig. 4 – Meshed workpiece reproducing microstructure of bone (Hage and Hamade, 2013).

material model (the same used in Alam (2009)). The properties of the bone are summarized in Table 1. Although the resultant force was found to reproduce accurately experimental results reported in Alam et al. (2009), the model is quite simple and further improvement of the micro-scale modelling of bone cutting is required.

2.4. *Discussion on modelling of orthogonal cutting*

The isotropic approach to bone behaviour uses the great experience in metal cutting simulation to reproduce bone cutting. Thus several authors have used typical constitutive models for metal alloys adapted to bone cutting. Although bone is clearly anisotropic also exhibits some plasticity and this is the reason for the success in simulating cutting with this approach. This approach allows using 2D simulation, which is a considerable advantage because of computational efficiency.

The anisotropy of bone, demonstrated in experimental studies, led to the development of models adapted from composite cutting modelling. This field of research is much more reduced than metal cutting simulation. It is worth noting the lack of simulation works in composite cutting capable to predict temperature variations (Santiuste et al., 2014). This is a reason explaining that few works have been found with an anisotropic approach to bone cutting. This approach requires 3D modelling, which is time consuming even for the simplest case of orthogonal cutting.

Also micro-scale modelling is poorly addressed. The development of this approach would allow predicting important features such as the role of the cement line, where usually the propagation of microcracks is located.

3. Drilling

Conventional bone drilling is extensively used in orthopaedics/traumatology and dentistry, although other no conventional cutting processes in bone are progressing, such as water jet (Dunnen et al., 2013). Frictional heat from conventional drilling may result in thermal necrosis of bone. It is worth noting that the nature of the drilling process makes it difficult the refrigeration and often causes thermal damage, even in the industrial manufacturing operations in metals and composites. The quality of the drilled hole where the fixation screw will be located should be free of damage in order to avoid osteonecrosis. The implant failure rate for leg osteo-synthesis ranges between 2% and 7% (Augustin et al., 2007) and it is higher than the failure rate for upper limbs due to physiologic stress during locomotion.

The interest of thermal osteonecrosis due to bone drilling has motivated the development of recent reviews (Augustin et al., 2012; Pandey and Panda, 2013). Different aspects influencing temperature and surface quality were analysed: drill parameters including geometry, cutting material and coatings. Also cutting parameters such as feed rate, cutting speed and the use of coolant were evaluated. The measurement of temperature in drilling of bones and new trends in the field of bone drilling were included in those reviews. Most works available in the literature provide an experimental approach. The extensive number of variables involved complicates the statement of concluding remarks and corroborates the interest in developing predictive tools for bone drilling, poorly developed to date.

Not only temperature remains a challenge during drilling, but also the prediction of cutting forces is also important, since uncontrolled large forces can cause drill-bit breakage, drill breakthrough, excessive heat generation, and mechanical damage to the bone. Prediction of cutting forces is required for the development of realistic training tools for surgery. The advent of haptic simulation systems for orthopaedic surgery procedures has provided surgeons with an

excellent tool for training and preoperative planning purposes. Drilling is one of the operations requiring extensive training because of the difficulties arising from vibration and the risk of drill bit breakage (Tsai et al., 2007). Proper simulation of the process requires accurate prediction of visual issues and also reproducing the sense of touch. The former aspect has received much more attention, see for instance (Niu et al., 2008). However force prediction has been poorly analysed in the literature.

The works reviewed in this paper are grouped into subsections in order to give the reader a clear vision of the state of the art. Mechanistic and analytical models are presented first. Analytical modeling of drilling commonly involves a simplification of the problem. Secondly the models giving a thermal approach are presented. This approach uses FE modeling mainly to simulate heat propagation in the workpiece and substituting the drilling process by a heat source. Finally the simulation of chip removal is reviewed.

3.1. *Mechanistic and analytical models*

Drilling is a cutting process combining tool rotation and the penetration into the workpiece. The drill has a complex geometry, optimized for the current operation and it is required to reproduce all details if accuracy in simulation is desired. The complexity of finite element models has motivated the development of analytical and mechanistic models based on extensive experimentation. Even in the case of metal and composite drilling, it is difficult to find accurate numerical models due to the above difficulties and the high computational cost involved in simulation of the drilling process (Feito et al., 2014).

Lee et al. (2012) developed a mechanistic force model for prediction of thrust force and torque during bone drilling. The model includes analytical calculations of drill-bit parameters, cutting conditions, and cutting geometry, while taking the material and friction properties into account through empirical specific energies. Only a small number of tests were needed to calibrate the specific energies for a broad range of drilling conditions and drill-bit geometries.

Sui et al. (2014) improved the model developed by Lee et al. (2012) to predict the thrust force and torque when drilling the bovine bone material. The cutting action at the drill point was divided into three distinct regions: the cutting lips, secondary cutting edges, and indentation zone. Thus, different models were formulated to consider the cutting mechanics of each region. The model was calibrated for bovine cortical bone and validated for a wide range of spindle speeds and feed rates. The predicted results agreed well with the experimental results. The limitations of the model include the calibration experiments to determine the coefficients for specific cutting pressures, the extension of the specific cutting pressures to the secondary cutting edges, and the assumption of a plastic extrusion mechanism for the bone in the indentation zone.

3.2. *Thermal models*

Davidson and James (2003) developed an analytical model based on machining theory in order to predict heat generation involved in drilling. The model was coupled with a further numerical simulation of heat transfer based on FE aiming at predicting the temperature field in bone during a drilling operation. The influence of the rotational speed, feed rate, drill geometry and bone material properties on the temperature rise was analysed in a parametric analysis. The most influencing variables are drill speed, feed rate and drill diameter while variations in drill helix angle, point angle and bone thermal properties have relatively little effect. The authors explain that the model appears to be realistic at low to moderate drill speeds, but it is not consistent with experimental evidence at high drill speeds. The most probable cause is improper modelling of bone failure at high speeds.

A similar thermal model for cortical bone drilling (bovine femur) was developed by Lee et al. (2011) combining a unique heat-balance equation in the drill bit-chip stream system, an ordinary heat diffusion equation in the bone, and heat generation at the drill-bit tip based on established machining theory. The model was solved numerically, using a tailor-made finite-difference scheme for the drill bit–chip stream system, coupled with a classic finite difference method for the bone. The influence of cutting parameters (cutting speed, feed rate, drill-bit diameter, point angle, and helix angle) on the maximum temperature reached was analysed. The highest maximum temperatures were observed at high feed rates, high point angles, and low helix angles, being the most influencing parameters. Although the effect of spindle speed and drill diameter was not so manifest, high spindle speeds and small drill diameters were observed to lead to the highest maximum temperatures. These results do not agree with the results presented by Davidson and James (2003). The differences could be related to the different ranges of spindle velocity considered; much higher in the case of Davidson and James (2003), in the range 50.000–200.000 rpm, than those analysed in the work of Lee et al. (2011) in the range 400–3000 rpm. When the cutting speed is high enough the process can be considered quasi adiabatic and the heat generated at the primary zone is mostly evacuated with the chip. Davidson and James (2003) also remark the differences between experiments and the model when the spindle velocity is increased.

Wang et al. (2014) analysed vibrational drilling of fresh bovine bones compared to conventional drilling using experimental and finite element approach in order to investigate the temperature induced in both processes. The experimental results showed that, compared with the conventional drilling, vibrational drilling could significantly reduce the cutting temperature in drilling of cortical bone. Concerning the numerical model, only the heat conduction between the drill bit and the bone was simulated. To verify the finite element model, temperatures of the drill bit were obtained just after drilling from the experiment, then the mean temperature was assigned to the outer wall of the drill bit model. A two-dimensional finite element model (FEM), which was generated by the pre-processing software GAMBIT along with the CFD software FLUENT was used to simulate the cutting heat conduction. They found that there is a downward trend of the cutting temperature with an increase of vibration frequency and amplitude. The authors concluded that vibration drilling can reduce the cutting heat in cortical bone drilling.

3.3. *Chip removal modelling*

The need to reproduce the complex tool geometry in drilling requires the development of three dimensional (3D) FE

approaches. The main drawback of the 3D modeling is the elevated computational cost especially because a great number of small elements are required in order to reproduce the temperature gradient at the machined surface and beneath this zone. Some efforts have recently been done in the application of this modelling technique to the analysis of bone drilling.

Lughmani et al. (2013) developed a 3D finite element (FE) model for the prediction of thrust forces experienced during cortical bone drilling (bovine femur). The model, developed in the commercial code ABAQUS/Explicit, incorporates the dynamic characteristics involved in the process along with the accurate geometrical considerations. It also allows the simulation of chip removal. The cortical bone in this study was modelled as a transversely isotropic material and an elastic–plastic law was used for the material constitutive model. The high strain rate data were obtained by using Split Hopkinson Pressure Bar (SHPB) experiments. A simple erosion criterion was stated as the maximum level of the equivalent plastic strain above which mesh elements were erased. The mechanical properties used in finite element analysis are included in the summary presented in Table 1. The FE model predicted the drilling thrust force and torque with reasonable accuracy when compared to experimental results. The validated drilling model was used to determine the thrust force and torque for different drilling conditions. It was observed that the thrust force and torque increased with an increase in the feed rate and spindle speed.

Sezek et al. (2012) developed a FE model using the MSC system in order to predict temperature change during cortical bone drilling (bovine tibia), see Fig. 5. Remeshing was used in order to prevent the mesh impairment due to chip formation during drilling. The bone was assumed to behave as an elastic isotropic material; thermo-mechanical properties used by the authors are given in Table 1.

The authors concluded that not only cutting parameters influenced the maximum temperature, but also bone density has a significant effect (the applied drill force increased as bone density increased; temperature increased 10% with a 12% increase in bone density). This fact should be accounted for when defining feed-rate and drill rotation speed in order to minimise the necrosis.

Tu et al. (2013) developed a temperature–displacement coupled FE model to simulate the thermomechanical behaviour of the contact region between the drill bit and bone analogue. The dynamic simulations were performed using the commercial ABAQUS/Explicit code. The model included both cortical and cancellous zones. The mechanical behaviour of the bone analogue (cortical and cancellous) was assumed to be elastic–plastic (the corresponding properties of cortical and cancellous zones are included in Table 1).

A dynamic failure criterion was applied to control the element removal during the drilling operation. Element deletion and mass scaling were employed to enable convergence of the FEM solution in the drilling modelling avoiding distortion and an excessive computational cost. The thermal contact behaviour between the drill bit and bone was modelled using surface-to-surface contact discretization. The friction behaviour between the drill bit and bone was assumed to be governed by Coulomb's friction law, with a coefficient of friction equal to 0.3.

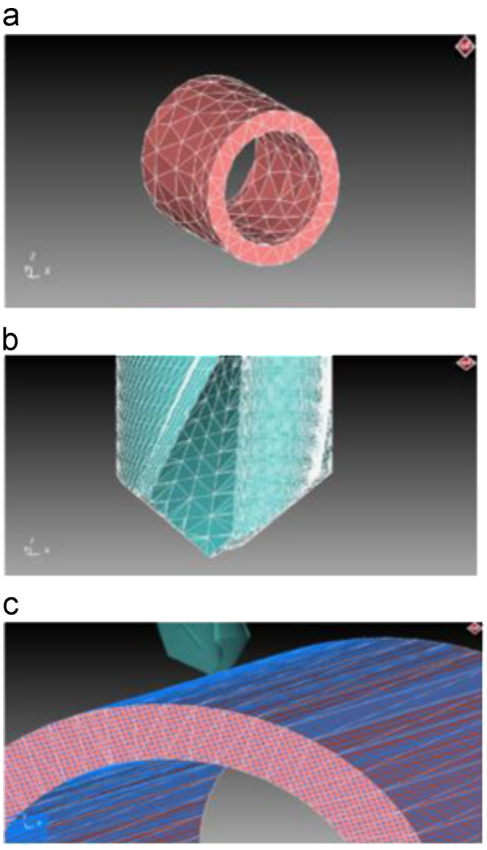

Fig. 5 – Drilling model developed by Sezek et al. (2012). (a) Bone model and mesh; (b) mesh for drill point; and (c) distribution of stress point locations in bone modelling used in FEM analysis.

The peak bone temperature and the size of the thermally affected zone were found to increase with enhancing drilling speed. The FE model was verified by experiments and was used to predict the peak value of the bone temperature during drilling with speeds of 600, 800 and 1200 rpm. Good accuracy in temperature predictions was achieved, with differences less than 3 °C between the peak temperature calculated with FE model and measured from the experiments. The range of velocity is not wide in this work and it would be interesting to check the behaviour of the temperature and the size of the thermally affected zone for higher values of the velocity. Probably these parameters would tend to stabilize when the spindle velocity is high enough.

3.4. *Discussion on drilling models*

Complete modelling of drilling is difficult. Even in the well-known field of metal, it is hard to find complete models of drilling including chip removal simulation. In the case of composite drilling, the development of anisotropic models for composites in complex cutting processes such as drilling has been recently reported in the literature (Feito et al., 2014). The advantage of this type of models is the possibility of predicting cutting forces, temperature and mechanical damage. The latter aspect is crucial in composites, being delamination the main defect induced during drilling. In the case of bone

cutting, all works dealing with chip removal in bone drilling assume an isotropic behaviour of bone with a simple constitutive equation.

The complexity of the 3D modelling required for chip removal reproduction has motivated the development of thermal models oriented to the prediction of temperature. Despite cutting forces and mechanical damage cannot be predicted with these models, the temperature field is a valuable information.

Also mechanistic models have been developed in order to identify the most influencing parameters on temperature rise. Setting cutting parameters is not always a defined issue and these models can help when it comes to decide cutting conditions.

It is clear the necessity of improvement of models available for drilling simulation. However, the elevated computational cost of the complete 3D approach is the major drawback.

4. Grinding and milling

Grinding and milling are also used in surgery, although there are only few works dealing with modelling of these processes. Even in the case of industrial processes, the modelling of grinding and milling of structural materials is not extensively developed.

Grinding is commonly used in surgery involving plane bones. For instance bone grinding using a miniature spherical diamond wheel (also called bur) is a common procedure in the expanded endonasal approach for brain cancer treatment in the skull base. Patients suffering from malignancies of the ventral and ventral-lateral skull base often require radical surgical resection of the tumour. The advent of endoscopic technology first in otolaryngology and subsequently in neurosurgery allowed the use of a transnasal route to access the skull base. This technique avoids facial and scalp incisions and reduces the need to surgically remove healthy tissue (Nogueira et al., 2010).

Milling is involved in surgery requiring accurate machining of bone surfaces, for instance in the total knee arthroplasty. The accuracy of the location and orientation of the surgical cuts of the bone surfaces of tibia and femur is crucial to obtain proper joint kinematics and ligament balancing (Denis et al., 2001; Sugita et al., 2009b).

4.1. *Grinding*

Tai et al. (2013) proposed a concept to predict accurately bone temperature during neurosurgical grinding process based on a heat conversion model and an FE thermal model. Experimental results demonstrated the linear correlation between the motor electrical power and heat generation. The thermal model is built in the FE software ABAQUS using the converted heat source as the input to calculate the temperature distribution around the diamond bur bit. The spherical grinding bur was discretized into several elemental grinding wheels and it was assumed that each one conducted individual grinding. Since this was a moving heat source problem, the elements were removed sequentially toward the feeding direction to expose another round pattern for the next time step, as shown in Fig. 6. Although part of the heat is evacuated with chip removal, it was assumed to be negligible since the material removal rate is small in grinding. The FE thermal model, considering spherical bone-tool contact interface and material removal, demonstrated an accurate prediction of the temperature.

4.2. *Milling*

Shin and Yoon (2006) developed an analytical model based on a moving heat source for simulation of round bur milling. The fresh-milled surface temperature was measured using two infrared thermometers and the maximum temperature was extrapolated by a moving plane heat source solution.

The estimated maximum temperature increment varied from 49 to 115 °C under various cutting conditions. These results showed that the thermal damage may reach about 2 mm in depth during round bur milling. A larger feed rate and a smaller cutting depth decreased the maximum temperature.

A similar approach was used by Sugita et al. (2009b) to analyse the temperature distribution during end milling of cortical pig bone. The temperature distribution inside the bone

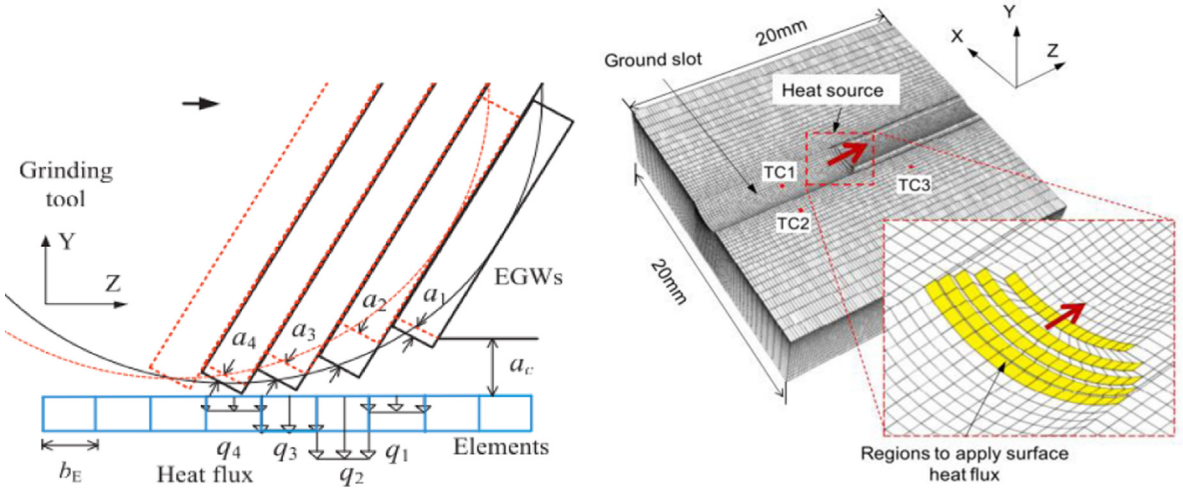

Fig. 6 – Thermal model reproducing bone grinding developed by Tai et al. (2013).

was calculated theoretically using a linear heat source moving on a semi-infinite plane. Analytical and experimental results indicate that bone within 0.1 mm of the surface layer may be injured by thermal damage caused by the cutting heat.

4.3. *Discussion on grinding and milling models*

Few works focusing on grinding and milling were found in the literature. The approaches involve thermal modelling of the heat propagation once the heat source was established. Thus the chip removal process (generating heat due to friction and workpiece deformation) was substituted by a moving heat source, calculating the heat with different simplifying hypotheses. It is difficult to extract general conclusions concerning penetration of thermal damage since it is dependent on the process parameters, tool geometry and other factors.

The development of grinding models including chip removal is still a challenge even in metal cutting. It is important to note the scale of the problem involving small chips and, therefore, the validity of common constitutive models used for metals in the macroscale is not clear. Moreover 3D analyses, with high computational cost are required. These problems have motivated the use of thermal models in metal alloy grinding.

Concerning milling, it is also a complex process, involving alternative cutting and variable chip section. It is possible to find models simulating chip removal in metal cutting, but again the computational cost is the main drawback. The lack of works dealing with modelling of these complex processes in composite cutting is also remarkable.

In summary, further developments in the numerical modelling of bone grinding and milling are still needed.

5. Other processes

The fracture of bone due to indentation with a hard, sharp object is of significance in surgical techniques and certain trauma situations. Although indentation is not commonly considered as a cutting process it is briefly reviewed in this section due to its importance in surgery. Penetration is close to machining because of the common entrance of one body (tool) in other (workpiece). Penetration mechanics is also involved in dynamic processes such as impact. Despite the interest of impact phenomena, they are out of the scope of this work.

5.1. *FE assuming isotropic behaviour*

The halo fixator, introduced in 1959 for immobilization of the cervical spine (Perry and Nickel, 1959) is a good example of surgical technique requiring penetration. It is used for immobilization and traction during surgical procedures and after injuries. Voor et al. (1997) developed an early FE study of stresses induced during halo pin insertion.

Halo pin insertion was modelled using nonlinear finite element analyses to determine the stress distribution in the human skull underlying and surrounding the point of pin fixation.

Bone behaviour was assumed to be elastic–plastic. Elastic properties of the human skull bone were based on the results of McElhaney et al. (1970) who found that the elastic constants of skull bone do not vary with direction within the plane of the skull surface. Elastic isotropy was used to represent human skull cortical bone (also in the outer cortical layer in the direction normal to the surface). The properties characterizing the bilinear elastic–plastic material behaviour were obtained from previous works in the literature (Reilly and Burstein, 1975; Wood, 1971, Cezayirlioglu et al., 1985; Davy and Connolly, 1982; Evans and Lissner, 1957; McElhaney et al., 1970) and they are summarized in Table 1.

The FE model solved in the code Abaqus was validated through the comparison with experimental penetration tests in terms of pin insertion depth and the profile of the hole generated in the bone. The region surrounding the pin tip within 1 mm was found to undergo plastic deformation and compressive loading in excess of the compressive yield strength of cortical bone. Damaged bone in this region seems to be responsible for the high incidence of halo pin loosening.

Kasiri et al. (2010) studied the fracture of bovine bone under indentation. Experiments were carried out and the theory of critical distances (TCDs) was used to predict failure due to cracking in the zones close to stress concentrations. Failure is assumed to occur when a characteristic stress reaches a critical value σ_0. The authors used the point method to predict the fracture force of indentation, the characteristic stress is simply the stress at a particular point $r=L/2$ where L is a material constant known as the critical distance. The failure criterion is formulated in the following equation:

$$\sigma(L/2) = \sigma_0 \tag{6}$$

Thus if the stress at a distance $L/2$ from the notch root reaches a critical value, failure will occur by crack propagation.

The fracture stress criterion is usually a combination of shear and normal stresses acting on the critical plane containing the crack, thus defining an effective stress as a simple scalar quantity. The authors used the Coulomb–Mohr criterion to model failure, assuming that the critical stress is a linear combination of the normal and shear stresses on the fracture line, as shown in Eq. (7). The equivalent critical stress is assumed to be the nominal shear strength τ_u as the equation is satisfied if there is no normal stress on the critical plane.

$$|\tau| + \alpha \cdot \sigma = \tau_u \tag{7}$$

where τ and σ are respectively, the shear and normal stresses, acting on the fracture plane. The value of shear strength was averaged from different works in the scientific literature $\tau_u = 73$ MPa.

The FE analysis of stress distribution was performed in the code ANSYS using two-dimensional plane strain models. The force–displacement curves obtained from experiments were employed for validation. Bone was modelled as an isotropic bilinear material with von Mises plasticity. To model the material in longitudinal, transverse, and tangential indentation directions, the following Young's moduli were used: 18 GPa, 10 GPa, and 8.5 GPa, respectively. These effective Young's moduli were obtained from compression tests on similar samples from the same source. The tangent modulus and yield stress of the material model were adjusted with the experimental force–displacement data. Indentation caused fracture of bone: failure occurred due to cracking along planes determined by the anisotropic structure of the material, governed by local shear stresses and inhibited by compressive stresses. Bone orientation has an influence on the fracture, being crack growth easier in

the tangential direction than in the longitudinal. Major cracks grow in the weakest possible structural direction.

5.2. *FE assuming anisotropic behaviour*

In a recent work Li et al. (2014) developed a new hybrid FE model using ABAQUS/Explicit based on a 3D smoothed-particle-hydrodynamic (SPH) domain included into a continuum FE one. This work focused on the characterization of the anisotropic deformation and damage behaviour of bovine cortical bone under a penetration process. The material properties used in the model were obtained in previous experimental works (Abdel-Wahab et al., 2011; Li et al., 2013a, 2013b, 2013c), see Table 1.

Experimental evidences showed a clear anisotropic behaviour of the cortical bone tissue and the influence of the underlying microstructure. The mechanical behaviour of the bovine cortical bone was modelled as a transversely isotropic elastic–plastic material incorporating the Hill's anisotropic yield criteria and progressive degradation. The yield surface is given by Eq. (8) being F, G, H, L, M and N phenomenological constants:

$$F(\sigma_y-\sigma_z)^2+\ G(\sigma_z-\sigma_x)^2+H(\sigma_x-\sigma_y)^2+2L\tau_{yz}^2+2M\tau_{xz}^2+2N\tau_{xy}^2=1 \tag{8}$$

The six Hill's constants used in the model were calculated based on the literature data in Reilly and Burstein (1975). The constants are included in Table 1.

Strain hardening for different directions was obtained from experimental observations (Li et al., 2013b). Criteria for damage initiation and evolution were stated from experimental data included in Mercer et al. (2006) and damage onset was assumed to occur when the strain reaches 2% (Li et al., 2013b). An energy-based criterion governed damage evolution, defining progressive degradation of the material through the decrease in the yield stress and stiffness degradation. It is assumed that damage in the specimen increases gradually up to its complete failure when the energy dissipated at damage evolution attains the critical level of energy release. A summary of material properties used in the numerical model developed by these authors is given in Table 1.

The anisotropic damage criteria employed in the models demonstrated its ability to reproduce the orientation-dependent damage features observed in the experiments (Fig. 7).

5.3. *Discussion on penetration models*

Indentation has been modelled using both isotropic and anisotropic approaches to mechanical behaviour of bone. Only few works are available in the literature. In some works penetration has been analysed under the point of view of crack propagation. Fracture mechanics can help in the understanding of bone cutting, as briefly discussed in next section.

6. Bone cutting and its relationship to fracture mechanics

The physical mechanisms involved in the above machining processes are ultimately related to the rupture of the material. In fact, during the last decade some research works, e.g. those led by Atkins and Williams (Atkins, 2003; Williams et al., 2010), have focused on the relationship between the machining forces and the fracture toughness G_c, i.e. the specific energy of rupture of the material, thus relating the machining processes and fracture mechanics.

Despite some controversy that neglects the importance of fracture versus plastic and friction mechanisms in cutting (Atkins, 2003), the consideration of mechanisms that involve fracture mechanics is not new (Reuleaux, 1900) and has been often thought as requiring the existence of a crack ahead the cutting tool, such as those observed in Fig. 2 for cortical bone (Sugita et al., 2009a). For the cases shown in Fig. 2, it is evident that the combination of shear forces ahead the cutting tool plus normal tensile forces leads to the local breakage of bone tissue. Both types of actions should be taken into account simultaneously and can be interpreted as local mode II (shear mode) and mode I (normal mode) of fracture. Wiggins and Malkin (1978) proposed a fracture based chip formation model in the orthogonal machining of bone and Kishawy et al. (2004) considered the energy of fracture for the interfacial debonding of particles in the orthogonal cutting of metal matrix composites. Atkins (2003, 2005) firmly established that the fracture terms are important in any cutting analysis. Atkins (2005) presents an excellent introduction to the mechanics of the cutting problem and justifies the need of considering the fracture toughness of the material in the energy balance. A fact that proves the need of including fracture terms in the energy balance is that a separation criterion must be introduced in any finite element simulation of a cutting process to allow for a tool advance, Atkins (2003, 2005).

The presence of an observable crack is not a necessary condition to apply a fracture mechanics approach involving G_c to the cutting process, since the fracture work can be significant even when no obvious cracking is evident (Patel et al., 2009a; Williams et al., 2010; Atkins, 2003, 2005). Cracking ahead the tool tip can happen under non usual cutting conditions, such as large depths of cut with large rake angles. This leads to crack formation with a speed which is faster than the tool speed. This effect was also described in Astakhov (1999) as the cause of chip formation for brittle materials machined with positive rake angle tools. However, in other machining operations there is no observable crack because the tool speed and the crack surface formation speed coincide (Atkins, 2003).

Patel et al. (2009a) give a detailed analysis for the estimation of G_c from orthogonal cutting machining tests and a very similar approach was reported previously by Atkins (2005). For the simplest case of plastic shearing at the chip formation plane (Williams et al., 2010) and the geometric configuration given in Fig. 8, they arrive to the following equation:

$$G_c=\frac{F_c}{b}-\sigma_Y\left(1+\frac{2}{\sigma_Y h}\frac{F_t}{b}\right)^{1/2} \tag{9}$$

where F_c is the applied cutting force (it is assumed that the tool moves at a constant speed), F_t is the reaction force on the tool (thrust force), b is the width of the work piece and h is the depth of cut. In the derivation of Eq. (9) a cutting force

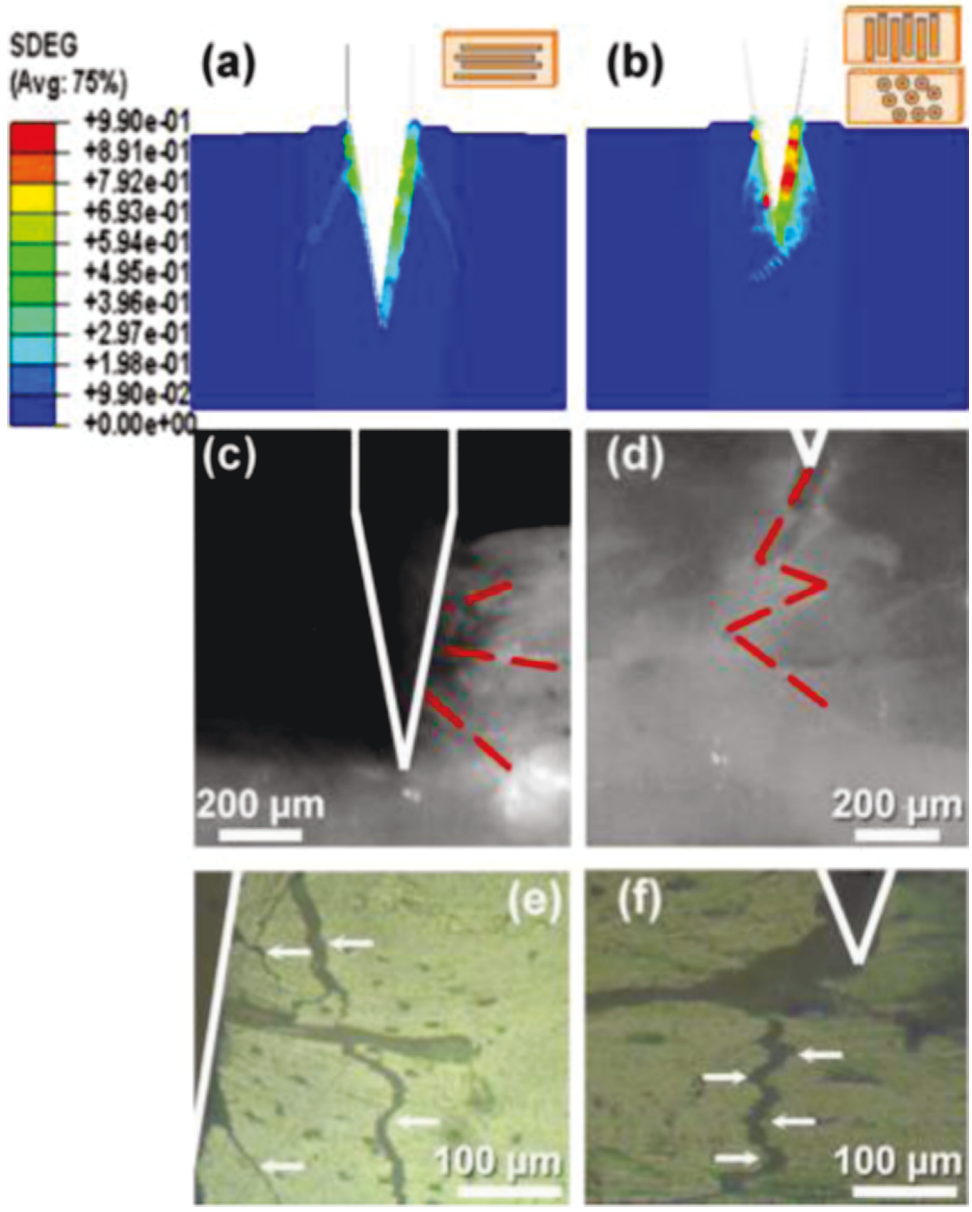

Fig. 7 – Comparison of simulation results (a and b) with images taken with high-speed camera (c and d) and optical microscopy (e and f) of damage induced by cutting along different directions: (a, c and e) perpendicular to bone axis, lateral damage propagation was observed; (b, d and f) parallel to bone axis, damage was in front of cutting tip. White lines designate the profile of razor blade, red dotted lines indicate crack lines and arrows point at the crack path (obtained from Li et al., 2014).

minimization approach (Merchant's force minimization criterion) is used (Patel et al., 2009b). On the other hand, σ_Y is the tensile yield stress, which in principle is also an unknown value. In Patel et al. (2009a), σ_Y refers to the ultimate average shear stress occurring at the shear plane forming an angle ϕ in ductile materials. Patel et al. (2009a) propose to perform a set of experiments in which F_c/b and F_t/b are measured for a range of h values (depths of cut). Then G_c and σ_Y may be found simultaneously using an iterative procedure. Note that this approach does not require information regarding the friction condition. These authors also report three other variants of the method to obtain G_c from cutting tests together with other magnitudes. Their results show a good agreement with the expected values.

In Williams et al. (2010) and Williams (2011) similar analyses are presented for other geometric configurations in which the tool tip does not need to touch the crack tip (i.e. the crack tip is ahead the tool tip). In addition to the case of plastic shearing described above, other geometric configurations include elastic bending and elastic–plastic bending of the chip that is being formed, with consideration of eventual chip curling, with and without crack tip touching. Note that crack tip touched by the tool tip as in Fig. 8 leads to direct transfer of a certain amount of energy from the cutting force to the fracture process (Williams, 2011).

References reviewed in previous sections show that a certain degree of ductility is expected in bone machining, see e.g., Childs and Arola (2011). In a recent work, Sui et al. (2013)

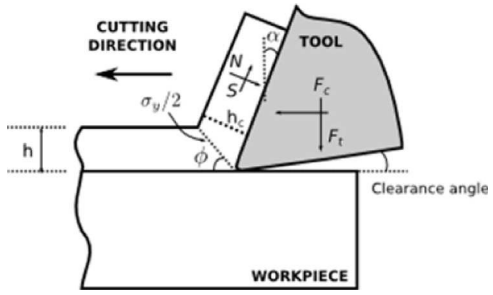

Fig. 8 – Geometry and forces acting in orthogonal cutting.

make use of a Merchant's analysis including a shear plane assumption as in Fig. 8 for orthogonal cutting tests of bovine cortical bone. Sugita et al. (2009a) also point out that when cutting cortical bone at depths of cut less than 20 μm a semi-continuous chip is observed. Furthermore, continuous chip formation is reported in orthogonal cutting of bovine cortical bone up to a depth of cut of 300 μm (Alam et al., 2013), and hence the above scheme for calculation of G_c can be applied.

In any case, yielding and chip formation in bone is not as manifest as for ductile metals (bone can be regarded as a quasi-brittle material, Cowin, 2001). Cracks can develop ahead the tool tip, such as in Fig. 2 and tend to appear when the depth of cut is large (Sugita et al., 2009a). In this case a modification of the procedure given in Patel et al. (2009a) could be derived from the energy balance and the applied cutting forces per unit width. The possibility of application of the procedure to brittle polymers is also reported in Patel et al. (2009a), for which small depths of cut produce steady-state cutting conditions. Atkins (2005) admits that this method can be applied to all materials displaying quasi-linear plots of cutting force vs. depth of cut under a continuous chip formation regime.

Yeager et al. (2008) noted that cracks in machining processes of bone can be developed in preferential directions, due to the anisotropy of the cortical tissue and the relatively low toughness perpendicular to the osteons. Sugita et al. (2009a) reported a very interesting study of the conditions that lead to microcrack generation for large depths of cut in bone. If the cutting force is less than 5 N, it is possible to control the crack length to less than 50 μm in all cutting directions. They studied the differences in the three anisotropic directions (see Fig. 2), concluding that the longest microcracks appear when cutting in the longitudinal direction (i.e. parallel to the osteon axis). In the across direction, cracks were observed to grow in a downward path from the cutting edge. In the transverse direction (osteons are perpendicular to the machined surface), cracks propagate easily around the osteons (cement lines).

An interesting case with potential application to bone cutting is the consideration of elastic behaviour of the material. If the energy release rate due to chip bending is small and can be neglected, then (Williams, 2011)

$$G_c = \frac{F_c}{b}(1 - \cos\theta) - \frac{F_t}{b}\sin\theta \tag{10}$$

where $\theta = \pi/2 - \alpha$ and α is the tool rake angle shown in Fig. 8. The derivation of the above equation takes into account the friction between chip and tool, which is the only source of dissipation considered in Eq. (10) (Williams, 2011). The effect of friction gives an apparent enhancement of the material toughness (Atkins, 2005) and that is the reason it results in subtracting terms in the computation of G_c in Eq. (10). Under the above conditions and for the hypothetical case of friction-less contact between chip and tool then G_c simply reduces to the following equation:

$$G_c = \frac{F_c}{b} \tag{11}$$

i.e., all the energy from the cutting force transfers to the fracture process (Atkins, 2005; Williams, 2011).

Despite the above approach is mainly focused on the machining of metals and polymers, it sets the basis for an extension to nonhomogeneous materials, such as bone. One of the main interests of this type of analysis is that it provides an indirect way of measuring G_c, which is an essential magnitude to model fracture processes and crack propagation at the micromechanics scale (Li et al., 2013a; Giner et al., 2014). In fact, fracture toughness of soft biological materials is currently determined by cutting using instrumented microtomes to record the cutting forces (Atkins, 2005). This is especially so for materials which are difficult to grip and from which it is difficult to manufacture standard test specimens.

In the case of bone, the standard quantification of G_c for the different bone phases, interfaces and anisotropy directions is very elusive and the values reported in the literature (see Li et al., 2013a) are sparse. These authors have also performed a thorough and systematic study of fracture toughness of bovine cortical tissue in different directions at the micro-scale (Li et al., 2013c). However, there is a need for more reliable and consistent estimations for ultimate strength and fracture values (Giner et al., 2014), e.g. for the cement line properties. Thus, cutting tests emerge as a potential complement for standard fracture toughness tests. In the case of metals and polymers, very good correlations have been reported (Patel et al., 2009a). Therefore, it is worth extending this approach to the case of bone to determine fracture toughness values, as acknowledged by Sui et al. (2013).

7. Machining of cancellous bone

Studies on cancellous bone machining are rarely found in the literature. Only one reference has been found concerning modelling of cutting of this tissue (Tu et al., 2013), already included in previous section. Some contributions focused on an experimental approach and these are summarized in this section.

Mitsuishi et al. (2004) developed a machine tool for total knee arthroplasty. They performed milling tests in cortical and trabecular bone. Cutting chips similar to powder were found just after the cutting of the mill in cancellous bone. The powder-like cutting chip results from the destruction of the cancellous bone in a brittle mode because it is spongy and therefore, the forces needed to break the trabeculae are very low. Fig. 9 shows chip formation during milling of cancellous bone.

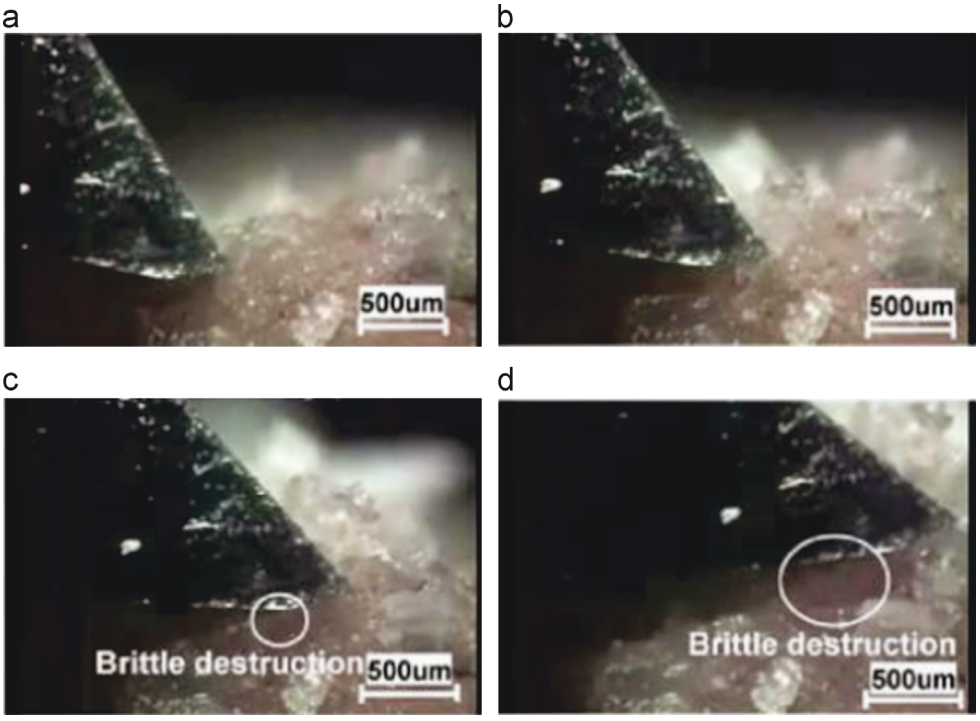

Fig. 9 – Cutting process of cancellous bone, obtained from Mitsuishi et al. (2004). (a) Tool rotation 0°; (b) Tool rotation 10°; (c) Tool rotation 20°; (d) Tool rotation 30°.

Jackson et al. (2005) analysed machining of cancellous bone prior to prosthetic implantation. They found that high strain rates change the mechanism of chip formation, thereby altering the shape of the chip. At high speeds chips are chunks of material rather than nicely formed chips. It is observed that the chip shape and its formation are less dependent on the material properties for high strain rates.

Malak and Anderson (2008) developed orthogonal cutting experiments on bovine cancellous bone in order to analyse the effect of tool rake angle, depth of cut and cutting speed on cutting forces, specific cutting energies and chip formation. They found that cancellous bone cutting is associated with bone marrow extrusion, which suggests damage to the bone architecture. Marrow extrusion was observed for all rake angles tested, and for depths of cut in the range of 1–3 mm. An increase in depth of cut resulted in a decrease of cutting energy, which was lower for large rake angles. Lower values of the rake angle produced discontinuous chips associated with severe fracturing that might be less favourable for cell survival. On the other hand, higher values of the rake angle promoted bone marrow extrusion and kept cutting energies low and little fracturing to the bone structure. These authors concluded that the viability of bone cells could be improved under conditions which promote large bone chips and low cutting energies.

It is worth noting the importance of improving knowledge on cutting processes of cancellous bone, not only for drilling operations involving penetrating through the cortical bone and inside the cancellous bone, but also for other surgical processes such as the autogenous bone graft harvesting. This process could result in cell death within the graft and trauma at the donor site and damage minimization requires a sound understanding of cutting process.

8. Conclusions and challenges

The bibliographic review included in this paper shows the main contributions in the field of numerical modelling of bone cutting.

From the review it is clear that attention in the literature is focused on cortical bone, with few works dealing with cutting of trabecular bone (a brief summary of experimental contributions is included). The improvement of knowledge concerning cutting of the latter tissue would be of valuable interest due to the current lack of information.

Concerning the modelling aspects, most works involve the FE method. In the case of very complex processes such as grinding and milling, some models only include thermal issues assuming the application of a heat source without simulation of chip removal. This approach is also commonly used in metal cutting especially in grinding, being difficult to find complete models that include chip removal.

In the case of drilling, this kind of approach is also used in some papers, but in other works chip removal is simulated. Simple constitutive models are used in drilling (isotropic, elastic–plastic). It is worth noting that in the case of other anisotropic materials such as composites, only few anisotropic complex models for drilling, including chip removal have been recently developed.

The complexity of the constitutive model increases when orthogonal cutting or indentation processes are modelled. It is worth mentioning that the modelling of these processes is relatively simple (sometimes they can be considered two dimensional), much more than machining processes involving tool rotation, and that has led to the proposal of more complex constitutive modelling including anisotropy.

Since the anisotropic nature of the bone has been evidenced, it seems that the development of 3D models of real machining operations in surgery including anisotropic constitutive modelling is one of the challenges in this field. However the computational cost of 3D approaches is one of the drawbacks that needs to be reduced.

Another challenge is related to the scale of the models, since most of them make use of a macroscopic approach. However, in order to model the mechanical damage it is necessary further developments at the micro-scale level.

Temperature is in most cases the focus of interest in modelling. The difficulty in measuring temperatures has motivated the development of models, but at the same time hindered their validation.

Fracture mechanics is related to cutting mechanisms and can help in the analysis of the mechanisms involved in bone machining. Further research is still necessary since up to the authors' knowledge no application of the fracture mechanics schemes to bone cutting has been reported yet in the literature.

Concerning the general validity of the results it is worth noting the differences between the conditions stated in the papers reviewed. The models simulated cutting processes, with different ranges of cutting parameters and the type of bone is not always the same, among other differences. In the case of models allowing chip removal the friction coefficient is related to the frictional heat generated at the interface chip/tool. However, the coefficient is different in the works analysed. Although the models reviewed have demonstrated their ability to reproduce experimental results developed in the same work or in the literature, it is difficult to obtain general conclusions because of the dispersion in the conditions established. Thus it is difficult to compare results and trends between the works analysed, even some contradictions are observed, probably due to the differences mentioned. In the case of models allowing chip separation simulation it is important to state realistic values of friction coefficient since cutting forces and heat generated are dependent on the level of friction. The value of friction coefficient also varies for the different works analysed being another source of discrepancy in the results.

In the authors' opinion, model predictions (cutting forces, thermomechanical damage) are still far from clinical application and a strong effort is still needed in the field of simulation of bone cutting processes.

Acknowledgements

The authors acknowledge to the Ministry of Economy and Competitiveness of Spain the financial support for this work received through the projects DPI2011-25999 and DPI2013-46641-R.

References

Abdel-Wahab, A.A., Alam, K., Silberschmidt, V.V., 2011. Analysis of anisotropic viscoelastoplastic properties of cortical bone tissues. J. Mech. Behav. Biomed. Mater. 4, 807–820.

Augustin, G., Davila, S., Mihoci, K., Udiljak, T., Vedrina, D.S., Antabak, A., 2007. Thermal osteonecrosis and bone drilling parameters revisited. Arch. Orthop. Trauma Surg. 128, 71–77.

Alam, K., 2009. Experimental and Numerical Analysis of Conventional and Ultrasonically-assisted Cutting of Bone. Doctoral Thesis, Loughborough University, Loughborough, UK.

Alam, K., Mitrofanov, A.V., Silberschmidt, V.V., 2009. Finite element analysis of forces of plane cutting of cortical bone. Comput. Mater. Sci. 46, 738–743.

Alam, K., Mitrofanov, A.V., Silberschmidt, V.V., 2010. Thermal analysis of orthogonal cutting of cortical bone using finite element simulations. Int. J. Exp. Comput. Biomech. 1, 236–251.

Alam, K., Khan, M., Silberschmidt, V.V., 2013. Analysis of forces in conventional and ultrasonically assisted plane cutting of cortical bone. Proc. Inst. Mech. Eng. Part H: J. Eng. Med. 227 (6), 636–642.

Alto, A., Pope, M.H., 1979. On the fracture toughness of equine metacarpi. J. Biomech. 12, 415–421.

Astakhov, V., 1999. Metal Cutting Mechanics. CRC Press, USA.

Atkins, A.G., 2003. Modelling metal cutting using modem ductile fracture mechanics: quantitative explanations for some longstanding problems. Int. J. Mech. Sci. 45 (2), 373–396.

Atkins, A.G., 2005. Toughness and cutting: a new way of simultaneously determining ductile fracture toughness and strength. Eng. Fract. Mech. 72, 849–860.

Augustin, G., Zigman, T., Davila, S., Udilljak, T., Staroveski, T., Brezak, D., Babic, S., 2012. Cortical bone drilling and thermal osteonecrosis. Clin. Biomech. 27, 313–325.

Bell, K.L., Loveridge, N., Power, J., Garrahan, N., Meggitt, B.F., Reeve, J., 1999. Regional differences in cortical porosity in the fractured femoral neck. Bone 24, 57–64.

Bigley, R.F., Griffin, L.V., Christensen, L., Vandenbosch, R., 2006. Osteon interfacial strength and histomorphometry of equine cortical bone. J. Biomech. 39 (9), 1629–1640.

Cezayirlioglu, H., Bahniuk, E., Davy, D.T., Heiple, K.G., 1985. Anisotropic yield behaviour of bone under combined axial force and torque. J. Biomech. 18, 61–69.

Childs, T.H.C., Arola, D., 2011. Machining of cortical bone: Simulations of chip formation mechanics using metal machining models. Mach. Sci. Technol. 15 (2), 206–230.

Cowin, S.C. (Ed.), 2001. Bone Mechanics Handbook. CRC Press, Boca Raton, Florida.

Davidson, S.R.H., James, D.F., 2000. Measurement of thermal conductivity of bovine cortical bone. Med. Eng. Phys. 22, 741–747.

Davidson, S.R.H., James, D.F., 2003. Drilling in bone: modeling heat generation and temperature distribution. J. Biomech. Eng. 125, 305–314.

Davy, D.T., Connolly, J.F., 1982. The biomechanical behaviour of healing canine radii and ribs. J. Biomech. 15, 235–247.

Denis, K., Van Ham, G., Vander Sloten, J., Van Audekercke, R., Van der Perre, G., De Schutter, J., Kruth, J.-P., Bellemans, J., Fabry, G., 2001. Influence of bone milling parameters on the temperature rise, milling forces and surface flatness in view of robot-assisted total knee arthroplasty. Int. Congr. Ser. 1230, 300–306.

Dunnen, S.D., Mulder, L., Kerkhoffs, G.M.M.J., Dankelman, J., Tuijthof, G.J.M., 2013. Waterjet drilling in porcine bone: the effect of the nozzle diameter and bone architecture on the hole dimensions. J. Mech. Behav. Biomed. Mater. 27, 84–93.

Evans, F.G., Lissner, H.R., 1957. Tensile and compressive strength of human parietal bone. J. Appl. Phys. 10, 493–497.

Feito, N., López-Puente, J., Santiuste, C., Miguélez, H., 2014. Numerical prediction of delamination in CFRP drilling. Compos. Struct. 108, 677–683.

Fox, M.J., Scarvell, J.M., Smith, P.N., Kalyanasundaram, S., Stachurski, Z.H., 2013. Lateral drill holes decrease strength of

the femur: an observational study using finite element and experimental analyses. J. Orthop. Surg. Res., 8–29.
Giner, E., Arango, C., Vercher, A., Fuenmayor, F.J., 2014. Numerical modeling of the mechanical behaviour of an osteon with microcracks. J. Mech. Behav. Biomed. Mater. 37, 109–124.
Guo, X.E., Liang, L.C., Goldstein, S.A., 1998. Micromechanics of osteonal cortical bone fracture. J. Biomech. Eng. 120, 112–117.
Hage, I.S., Hamade, R.F., 2013. Micro-FEM orthogonal cutting model for bone using microscope images enhanced via artificial intelligence. Procedia CIRP 8, 385–390.
Hogan, H.A., 1992. Micromechanics modeling of Haversian cortical bone properties. J. Biomech. 25, 549–556.
Hou, J.P., Petrinic, N., Ruiz, C., Hallett, S.R., 2000. Prediction of impact damage in composite plates. Compos. Sci. Technol. 60, 228–273.
Huiskes, J., 1980. Some fundamental aspects of human joint replacement. Acta Orthop. Scand. Suppl. 185, 44–108.
Jackson, M.J., Robinson, G.M., Sein, H., Ahmed, W., Woodwards, R., 2005. Machining cancellous bone prior to prosthetic implantation. J. Mater. Eng. Perform. 14 (3), 293–300.
Jacobs, C.H., Pope, M.H., Berry, J.T., Hoaglund, F., 1974. A study of the bone machining process – orthogonal cutting. J. Biomech. 7 (2), 131–136.
James, T.P., Chang, G., Micucci, S., Sagar, A., Smith, E.L., Cassidy, C., 2014. Effect of applied force and blade speed on histopathology of bone during resection by sagittal saw. Med. Eng. Phys. 36 (3), 364–370.
Johnson, W.M., Rapoff, A.J., 2007. Microindentation in bone: hardness variation with five independent variables. J. Mater. Sci.: Mater. Med. 18, 591–597.
Kasiri, S., Reilly, G., Taylor, D., 2010. Wedge indentation fracture of cortical bone: experimental data and predictions. J. Biomech. Eng. 132, 081009-1–081009-6.
Katz, J.L., Yoon, H.S., Lipson, S., Maharidge, R., Meunier, A., Christel, P., 1984. The effects of remodelling on the elastic properties of bone. Calcif. Tissue Int. 36, 31–36.
Keaveny, T.M., Morgan, E.F., Yeh, O.C., 2004. Bone mechanics. Stand. Handb. Biomed. Eng. Des., 1–24.
Kim, S.H., Chang, S.H., Jung, H.J., 2010. The finite element analysis of a fractured tibia applied by composite bone plates considering contact conditions and time-varying properties of curing tissues. Compos. Struct. 92, 2109–2118.
Kishawy, H.A., Kannan, S., Balazinski, M., 2004. An energy based analytical force model for orthogonal cutting of metal matrix composites. CIRP Ann. 53/1, 91–94.
Krause, W.R., 1987. Orthogonal bone cutting: saw design and operating characteristics. J. Biomech. Eng. 109 (3), 263–271.
Lee, J.E., Rabin, Y., Ozdoganlar, O.B., 2011. A new thermal model for bone drilling with applications to orthopaedic surgery. Med. Eng. Phys. 33, 1234–1244.
Lee, J.E., Gozen, B.A., Ozdoganlar, O.B., 2012. Modeling and experimentation of bone drilling forces. J. Biomech. 45 (6), 1076–1083.
Li, S., Abdel-Wahab, A., Demirci, E., Silberschmidt, V.V., 2013a. Fracture process in cortical bone: X-FEM analysis of microstructured models. Int. J. Fract. 184, 43–55.
Li, S., Demirci, E., Silberschmidt, V.V., 2013b. Variability and anisotropy of mechanical behaviour of cortical bone in tension and compression. J. Mech. Behav. Biomed. Mater. 21, 109–120.
Li, S., Abdel-Wahab, A., Silberschmidt, V.V., 2013c. Analysis of fracture processes in cortical bone tissue. Eng. Fract. Mech. 110, 448–458.
Li, S., Abdel-Wahab, A., Demirci, E., Silberschmidt, V.V., 2014. Penetration of cutting tool into cortical bone: Experimental and numerical investigation of anisotropic mechanical behaviour. J. Biomech. 47 (5), 1117–1126.
Lughmani, W.A., Bouazza-Marouf, K., Ashcroft, I., 2013. Finite element modeling and experimentation of bone drilling forces. J. Phys. Conf. Ser., 451.
Malak, S.F., Anderson, I.A., 2008. Orthogonal cutting of cancellous bone with application to the harvesting of bone autograft. Med. Eng. Phys. 30, 717–724.
Martin, R.B., Boardman, D.L., 1993. The effects of collagen fiber orientation, porosity, density, and mineralization on bovine cortical bone bending properties. J. Biomech. 26, 1047–1054.
Martin, R.B., Gibson, V.A., Stover, S.M., Gibeling, J.C., Griffin, L.V., 1996. Osteonal structure in the equine third metacarpus. Bone 19, 165–171.
McElhaney, J.H., Fogle, J.L., Melvin, J.W., Haynes, R.R., Roberts, V.L., Alem, N.M., 1970. Mechanical properties of cranial bone. J. Biomech. 3, 495–511.
Mercer, C., He, M.Y., Wang, R., Evans, A.G., 2006. Mechanisms governing the inelastic deformation of cortical bone and application to trabecular bone. Acta Biomater. 2, 59–68.
Merchant, M.E., 1945a. Mechanics of the metal cutting process. I. Orthogonal cutting and a Type 2 chip. J. Appl. Phys. 16 (5), 267–275.
Merchant, M.E., 1945b. Mechanics of the metal cutting process. II. Plasticity conditions in orthogonal cutting. J. Appl. Phys. 16 (6), 318–324.
Miguélez, H., Soldani, X., Molinari, A., 2013. Analysis of adiabatic shear banding in orthogonal cutting of Ti alloy. Int. J. Mech. Sci. 75, 212–222.
Mitsuishi, M., Warisawa, S., Sugita, N., 2004. Determination of the machining characteristics of a biomaterial using a machine tool designed for total knee arthroplasty. Ann. CIRP 53 (1), 107–112.
Mitsuishi, M., Warisawa, S., Sugita, N., Suzuki, M., Moriya, H., Hashizume, H., Fujiwara, K., Abe, N., Inoue, H., Kuramoto, K., Inoue, T., Nakashima, Y., Tanimoto, K., 2005. A study of bone micro-cutting characteristics using a newly developed advanced bone cutting machine tool for total knee arthoplasty. Ann. CIRP 54 (1), 41–46.
Molinari, A., Cheriguene, R., Miguelez, H., 2012. Contact variables and thermal effects at the tool–chip interface in orthogonal cutting. Int. J. Solids Struct. 49, 3774–3796.
Moyle, D.D., Welborn 3rd, J.W., Cooke, F.W., 1978. Work to fracture of canine femoral bone. J. Biomech. 11, 435–440.
Niu, Q., Chi, X., Leu, M.C., Ochoa, J.A., 2008. Image processing, geometric modeling and data management for development of a virtual bone surgery system. Comput. Aided Surg. 13 (1), 30–40.
Nobakhti, S., Limbert, G., Thurner, P.J., 2014. Cement lines and interlamellar areas in compact bone as strain amplifiers – contributors to elasticity, fracture toughness and mechanotransduction. J. Mech. Behav. Biomed. Mater. 29, 235–251.
Nogueira, J.F., Stamm, A., Vellutini, E., 2010. Evolution of endoscopic skull base surgery, current concepts, and future perspectives. Otolaryngologic Clin. North Am. 43, 639–652.
Nordin, M., Frankel, V.H., 2001. Basic Biomechanics of the Musculoskeletal System, 3rd ed. Lippincott Williams & Wilkins, USA.
O'Brien, F.J., Taylor, D., Lee, T.C., 2007. Bone as a composite material: The role of osteons as barriers to crack growth in compact bone. Int. J. Fatigue 29, 1051–1056.
O'Mahony, A.M., Williams, J.L., Spencer, P., 2001. Anisotropic elasticity of cortical and cancellous bone in the posterior mandibible increases peri-implant stress and strain under oblique loading. Clin. Oral Implant. Res. 12 (6), 648–657.
Pandey, R.K., Panda, S.S., 2013. Drilling of bone: a comprehensive review. J. Clin. Orthop. Trauma4, 15–30.

Patel, Y., Blackman, B.R.K., Williams, J.G., 2009a. Measuring fracture toughness from machining tests. Proc. Inst. Mech. Eng. Part C J. Mech. Eng. Sci. 223 (12), 2861–2869.
Patel, Y., Blackman, B.R.K., Williams, J.G., 2009b. Determining fracture toughness from cutting tests on polymers. Eng. Fract. Mech. 76 (18), 2711–2730.
Perry, J., Nickel, V.L., 1959. Total cervical spine fusion for neck paralysis. J. Bone Jt. Surg. 41A, 37–60.
Pithioux, M., Lasaygues, P., Chabrand, P., 2002. An alternative ultrasonic method for measuring the elastic properties of cortical bone. J. Biomech. 35, 961–968.
Reilly, D.T., Burstein, A.H., 1974. The mechanical properties of cortical bone. J. Bone Jt. Surg. 56, 1001–1022.
Reilly, D.T., Burstein, A.H., 1975. The elastic and ultimate properties of compact bone tissue. J. Biomech. 8, 393–405.
Reuleaux, F., 1900. Über den Taylor Whiteschen Werkzeugstahl Verein sur Berforderung des Gewerbefleissen. Sitzungsberichte 79 (1), 179–220.
Rho, J.Y., Zioupos, P., Currey, J.D., Pharr, G.M., 1999. Variations in the individual thick lamellar properties within osteons by nano-indentation. Bone 25, 295–300.
Santiuste, C., Miguélez, H., Soldani, X., 2011. Out-of-plane failure mechanisms in LFRP composite cutting. Compos. Struct. 93, 2706–2713.
Santiuste, C., Rodríguez-Millán, M., Giner, E., Miguélez, H., 2014. The influence of anisotropy in numerical modeling of orthogonal cutting of cortical bone. Compos. Struct. 116, 423–431.
Sezek, S., Aksakal, B., Karaca, F., 2012. Influence of drill parameters on bone temperature and necrosis: a FEM modelling and in vitro experiments. Comput. Mater. Sci. 60, 13–18.
Shin, H.C., Yoon, Y.S., 2006. Bone temperature estimation during orthopaedic round bur milling operations. J. Biomech. 39, 33–39.
Singhranu, H., 1987. The thermal properties of human cortical bone: an in vitro study. Eng. Med. 16, 175–176.
Soldani, X., Santiuste, C., Muñoz-Sánchez, A., Miguélez, H., 2011. Influence of tool geometry and numerical parameters when modeling orthogonal cutting of LFRP composites. Compos. Part A 42, 1205–1216.
Stumme, L., Baldini, T., Jonassen, A., Bach, J., 2003. Emissivity of bone. Summer Bioengineering Conf., 25–29.
Sugita, N., Osa, T., Aoki, R., Mitsuishi, M., 2009a. A new cutting method for bone based on its crack propagation characteristics. CIRP Ann. – Manuf. Technol. 58, 113–118.
Sugita, N., Osa, T., Mitsuishi, M., 2009b. Analysis and estimation of cutting-temperature distribution during end milling in relation to orthopaedic surgery. Med. Eng. Phys. 31, 101–107.
Sui, J., Sugita, N., Ishii, K., Harada, K., Mitsuishi, M., 2013. Force analysis of orthogonal cutting of bovine cortical bone. Mach. Sci. Technol. 17, 637–649.
Sui, J., Sugita, N., Ishii, K., Harada, K., Mitsuishi, M., 2014. Mechanistic modelling of bone-drilling process with experimental validation. J. Mater. Process. Technol. 214, 1018–1026.
Tai, B.L., Zhang, L., Wang, A., Sullivan, S., Shih, A.J., 2013. Neurosurgical bone grinding temperature monitoring. Procedia CIRP 5, 226–230.
Taylor, D., Hazenberg, J.G., Lee, T.C., 2007. Living with cracks: damage and repair in human bone. Nat. Mater. 6, 263–268.
Tsai, M.D., Hsieh, M.S., Tsai, C.H., 2007. Bone drilling haptic interaction for orthopedic surgical simulator. Comput. Biol. Med. 37 (12), 1709–1718.
Tu, Y.K., Chen, L.W., Ciou, J.S., Chen, Y.C., 2013. Finite element simulations of bone temperature rise during bone drilling based on a bone analog. J. Med. Biol. Eng. 33 (3), 269–274.
Vercher, A., Giner, E., Arango, C., Tarancón, J.E., Fuenmayor, F.J., 2014. Homogenized stiffness matrices for mineralized collagen fibrils and lamellar bone using unit cell finite element models. Biomech. Model. Mechanobiol. 13 (2), 437–449.
Voor, M.J., Andersont, R.C., Hart, R.T., 1997. Stress analysis of halo pin insertion by non-linear finite element modelling. J. Biomech. 30 (9), 903–909.
Wang, Y., Cao, M., Zhao, X., Zhu, G., McClean, C., Zhao, Y., Fan, Y., 2014. Experimental investigations and finite element simulation of cutting heat in vibrational and conventional drilling of cortical bone. Med. Eng. Phys. 36 (11), 1408–1415.
Wiggins, K.L., Malkin, S., 1978. Orthogonal machining of bone. J. Biomech. Eng. 100 (3), 122–130.
Williams, J.G., Patel, Y., Blackman, B.R.K., 2010. A fracture mechanics analysis of cutting and machining. Eng. Fract. Mech. 77 (2), 293–308.
Williams, J.G., 2011. The fracture mechanics of surface layer removal. Int. J. Fract. 170, 37–48.
Wood, J.L., 1971. Dynamic response of human cranial bone. J. Biomech. 4, 1–12.
Yeager, C., Nazari, A., Arola, D., 2008. Machining of cortical bone: surface texture, surface integrity and cutting forces. Mach. Sci. Technol. 12, 100–118.
Yoon, H., Katz, J., 1976. Ultrasonic wave propagation in human cortical bone. II. Measurements of elastic properties and microhardness. J. Biomech. 9, 459–464.